Efficient implementation of the Gutzwiller variational method

Nicola Lanatà,[1] Hugo U. R. Strand,[1] Xi Dai,[2] and Bo Hellsing[1]
[1]*University of Gothenburg, SE-412 96 Gothenburg, Sweden*
[2]*Beijing National Laboratory for Condensed Matter Physics and Institute of Physics, Chinese Academy of Sciences, Beijing 100190, China*
(Received 31 July 2011; published 31 January 2012)

We present a self-consistent numerical approach to solve the Gutzwiller variational problem for general multiband models with arbitrary on-site interaction. The proposed method generalizes and improves the procedure derived by Deng *et al.* [Phys. Rev. B **79**, 075114 (2009)], overcoming the restriction to density-density interaction without increasing the complexity of the computational algorithm. Our approach drastically reduces the problem of the high-dimensional Gutzwiller minimization by mapping it to a minimization only in the variational density matrix, in the spirit of the Levy and Lieb formulation of density functional theory (DFT). For fixed density the Gutzwiller renormalization matrix is determined as a fixpoint of a proper functional, whose evaluation requires only ground-state calculations of matrices defined in the Gutzwiller variational space. Furthermore, the proposed method is able to account for the symmetries of the variational function in a controlled way, reducing the number of variational parameters. After a detailed description of the method we present calculations for multiband Hubbard models with full (rotationally invariant) Hund's rule on-site interaction. Our analysis shows that the numerical algorithm is very efficient, stable, and easy to implement. For these reasons this method is particularly suitable for first-principles studies (e.g., in combination with DFT) of many complex real materials, where the full intra-atomic interaction is important to obtain correct results.

DOI: 10.1103/PhysRevB.85.035133 PACS number(s): 78.20.Bh, 71.10.Fd

I. INTRODUCTION

In the 1960s Martin Gutzwiller published a series of papers[1–3] where he introduced a variational method for studying ferromagnetism in transition metals. His brilliant idea was to variationally determine a projected wave function represented as

$$|\Psi_G\rangle = \prod_{\mathbf{R}} \mathcal{P}_{\mathbf{R}} |\Psi_0\rangle , \tag{1}$$

where the local operators $\mathcal{P}_{\mathbf{R}}$ improve the noninteracting wave function $|\Psi_0\rangle$ in accordance with the on-site interaction by modifying the weight of local electronic configurations.

In spite of its simplicity, the average values of any operator on $|\Psi_G\rangle$ can be computed only numerically for realistic lattice models, e.g., using variational Monte Carlo.[4,5] For this reason, Gutzwiller introduced an approximate scheme, known as the Gutzwiller approximation, to compute these average values analytically. Successively, the development of dynamical mean field theory (DMFT)[6] has brought additional insights into the physical meaning of the Gutzwiller approximation. In fact, Metzner and Vollhardt showed that this approximation is exact in the limit of infinite coordination lattices,[7–9] where the single-particle self-energy becomes purely local in space.[10]

Since its introduction, the Gutzwiller wave function and approximation have proven to be very important tools to study strongly correlated systems. The understanding of many basic concepts, such as the Brinkman-Rice scenario for the Mott transition,[11] came originally from calculations based on the Gutzwiller method. From the computational point of view, the list of interesting results that have been obtained by means of the Gutzwiller approximation[1–3] and its respective generalizations[9,12–15] is impressively long and, hence, impossible to cite in an exhaustive way. Furthermore, the Gutzwiller approximation can be naturally combined with density functional theory (DFT),[16,17] applying, e.g., the local density approximation (LDA)[18] for the exchange and correlation. LDA + Gutzwiller (LDA + G)[19,20] has proven to be a powerful scheme for the study of real strongly -correlated metallic materials,[20] giving a more accurate description than LDA + U,[21] comparable to LDA + DMFT[22] for ground-state properties. Finally, the range of application of the Gutzwiller method has recently been extended to out-of-equilibrium calculations, such as electron transport across quantum dot systems[13,15] and quench dynamics in correlated electron systems.[14]

The Gutzwiller variational method requires a number of preliminary technical steps in order to make it really flexible and able to cope with systems of interest, as the number of variational parameters scales exponentially with the number of correlated orbitals involved in the calculation. This scaling is already problematic for transition-metal systems with correlated d orbitals if the required minimization is performed in a naive way. Based on the formalism introduced by Bünemann,[23] Deng *et al.*[20] recently derived a self-consistent numerical method that allows us to efficiently perform calculations even for d-orbital systems. The only limitation of this approach is the restriction to density-density types of interactions, which is actually due to the employed formalism and does not stem from the numerical approach in itself.

However, in order to properly describe the physics of several strongly correlated materials, the full intra-atomic interaction is needed, not only its density-density component. The rotational invariant on-site Coulomb and exchange interaction is generally modeled in terms of the so-called Kanamori parameters[24] commonly referred to with the symbols U and J. The strength of the two-electron spin-exchange interaction is determined by the parameter J. In transition-metal oxides with partly filled d shells the off-diagonal interactions—exchange coupling, spin flip, and pair hopping—are crucial. For example, the metallic property of $SrVO_3$ cannot be reproduced from theory without accounting for spin-exchange interaction.[25]

Several theoretical model studies points in the same direction. To mention a few, the transition from the paramagnetic to the ferromagnetic phase for multiband systems requires finite J,[23] the spin-freezing transition predicted for multiband systems, which is expected to influence the Mott transition,[26] takes place when $0 < J/U < 1/3$, and is absent for $J = 0$.[27] Previous Gutzwiller model studies[23] and the present work show that the critical U required for the Mott-insulator transition is substantially reduced when increasing the ratio J/U from zero.

Motivated by the above examples we believe that an implementation of the Gutzwiller variational method valid for general on-site interactions and, at the same time, numerically efficient would constitute an important step forward. Formal advancements pointing in this direction have lately been conceived by several authors,[23,28–34] although progress has been hampered by the lack of efficient numerical algorithms applicable to the most general case. In particular, Fabrizio and collaborators[30,32–36] derived a mathematical formulation of the problem whose complexity is unaffected by the form of the on-site interactions and, furthermore, allows us to easily incorporate symmetries into the variational function from the onset.

The main goal of this work consists of merging together the general formalism developed by Fabrizio and collaborators[30,32–35] mentioned above and the numerical procedure derived by Deng *et al.*,[20] overcoming the restriction to density-density interactions without increasing the complexity of the computational algorithm. Furthermore, the fully rotational invariant on-site interaction enables us to construct the variational wave function using the orbital rotational symmetry, which is instead broken if the off-diagonal terms are neglected. It will be shown that this extra symmetry can be used to reduce the number of variational parameters.

The outline of this paper is as follows. In Sec. II the Gutzwiller problem for a general tight-binding Hamiltonian is introduced. In Sec. III the employed formulation of the Gutzwiller method[30,32–34,36] is summarized. In particular, in Sec. III C it is shown that this formulation provides a natural extension of the formalism of Ref. 20, having the same mathematical structure in the special case of density-density on-site interactions. In Sec. IV we discuss the implementation of symmetries of the wave functions. In Sec. V the numerical procedure to minimize the Gutzwiller energy is described in detail. In Sec. VI we briefly discuss how the proposed method can be adapted to an LDA + G type of calculation. In Sec. VII we prove the reliability of the method, presenting a comparison with other methods for the cases of two and five orbitals. Furthermore, we discuss several technical details of the numerical procedure, such as convergence properties and computational speed. Finally, Sec. VIII is devoted to the conclusions.

II. THE GUTZWILLER METHOD

Let us consider the general tight-binding Hamiltonian

$$\hat{H} = \sum_{\mathbf{R}\neq\mathbf{R}'}\sum_{\alpha\beta} t^{\alpha\beta}_{\mathbf{R}\mathbf{R}'}\, c^{\dagger}_{\mathbf{R}\alpha} c_{\mathbf{R}'\beta} + \sum_{\mathbf{R}}\sum_{\Gamma\Gamma'} U(\mathbf{R})_{\Gamma\Gamma'}\, |\Gamma,\mathbf{R}\rangle\langle\Gamma',\mathbf{R}| \equiv \hat{T} + \hat{H}_{\mathrm{loc}}\,, \tag{2}$$

where $c^{\dagger}_{\mathbf{R}\alpha}$ creates an electron in state α (where α labels both the spin σ and the orbital a at site $\mathbf{R}$) and $|\Gamma,\mathbf{R}\rangle$ are many-body Fock states expressed in the $c_{\mathbf{R}\alpha}$ basis. These states are defined by the occupation numbers $n_\alpha(\Gamma,\mathbf{R}) \in \{0,1\}$, where α runs over integer numbers from 1 to M, M being the number of on-site single-particle states,

$$|\Gamma,\mathbf{R}\rangle = (c^{\dagger}_{\mathbf{R}1})^{n_1(\Gamma,\mathbf{R})}\ldots(c^{\dagger}_{\mathbf{R}M})^{n_M(\Gamma,\mathbf{R})}\,|0\rangle. \tag{3}$$

Thus, the number of Fock states is 2^M. The Hermitian matrix $U(\mathbf{R})$ represents the local terms, interaction and crystal fields, in the $c^{\dagger}_{\mathbf{R}\alpha}$ basis, i.e., the same basis in which $\hat{T}$ was defined in Eq. (2). This basis will henceforth be denoted as the *original* basis.

The structure of the Gutzwiller variational function is given by Eq. (1), where $|\Psi_0\rangle$ is an uncorrelated variational wave function that satisfies Wick's theorem and $\mathcal{P}_{\mathbf{R}}$ is a general operator acting on the local configurations at site $\mathbf{R}$

$$\mathcal{P}_{\mathbf{R}} = \sum_{\Gamma\Gamma'} \lambda(\mathbf{R})_{\Gamma\Gamma'}\, |\Gamma,\mathbf{R}\rangle\langle\Gamma',\mathbf{R}|\,, \tag{4}$$

where the $2^M \times 2^M$ matrix $\lambda(\mathbf{R})$, assumed to be real in this work, contains all the variational parameters needed to define the operator $\mathcal{P}_{\mathbf{R}}$.

In general, average values of operators with respect to $|\Psi_G\rangle$ must be computed numerically unless the lattice has an infinite coordination number, in which case they can be evaluated analytically if the following equations—commonly named Gutzwiller constraints—are satisfied:

$$\langle\Psi_0|\,\mathcal{P}^{\dagger}_{\mathbf{R}}\mathcal{P}_{\mathbf{R}}\,|\Psi_0\rangle = 1, \tag{5}$$

$$\langle\Psi_0|\,\mathcal{P}^{\dagger}_{\mathbf{R}}\mathcal{P}_{\mathbf{R}}\,\mathcal{C}_{\mathbf{R}}\,|\Psi_0\rangle = \langle\Psi_0|\,\mathcal{C}_{\mathbf{R}}\,|\Psi_0\rangle, \tag{6}$$

where $\mathcal{C}_{\mathbf{R}}$ is the local single-particle density-matrix operator with elements $c^{\dagger}_{\mathbf{R}\alpha}c_{\mathbf{R}\beta}$.

The variational problem to solve amounts to variationally determining both $|\Psi_0\rangle$ and $\mathcal{P}_{\mathbf{R}}$ by minimizing the average value of the Hamiltonian [Eq.(2)]

$$\mathcal{E}_{\mathrm{var}}[\mathcal{P},\Psi_0] = \langle\Psi_0|\,\mathcal{P}^{\dagger}\hat{H}\mathcal{P}\,\,|\Psi_0\rangle, \tag{7}$$

fulfilling Eqs. (5) and (6), where we have introduced

$$\mathcal{P} \equiv \prod_{\mathbf{R}} \mathcal{P}_{\mathbf{R}}. \tag{8}$$

For a general tight-binding model [Eq. (2)] this problem is complicated for two reasons: (i) $|\Psi_0\rangle$ and $\mathcal{P}$ are not independent variables because of the Gutzwiller constraints [Eqs. (5) and (6)] and (ii) the number of variational parameters scales exponentially with the number of orbitals.

III. REFORMULATION OF THE GUTZWILLER PROBLEM

In this section we briefly summarize the reformulation of the Gutzwiller problem derived in Refs. 33 and 34, and we show its formal analogy with the formulation of Bünemann and Weber[23] in the special case of pure density-density local interaction.

A. The mixed-basis representation

Let us introduce the so-called *natural-basis*[32] operators $d_{\mathbf{R}\alpha}$, i.e., the operators such that

$$\langle\Psi_0|\, d^\dagger_{\mathbf{R}\alpha} d_{\mathbf{R}\beta}\,|\Psi_0\rangle = \delta_{\alpha\beta}\, n^0_{\mathbf{R}\alpha} \equiv n^0_{\alpha\beta}(\mathbf{R}) \quad \forall\,\alpha,\beta, \tag{9}$$

where $0 \leqslant n^0_{\mathbf{R}\alpha} \leqslant 1$ are the eigenvalues of the local density matrix

$$\langle\Psi_0|\, c^\dagger_{\mathbf{R}\alpha} c_{\mathbf{R}\beta}\,|\Psi_0\rangle \equiv \bar{\rho}^0_{\alpha\beta}(\mathbf{R}). \tag{10}$$

Notice that the natural-basis operators are always well defined, as $\bar{\rho}^0(\mathbf{R})$ is Hermitian, implying that there always exists a unitary transformation $\mathcal{U}^{\mathbf{R}}$ such that

$$d^\dagger_{\mathbf{R}\alpha} = \sum_\beta \mathcal{U}^{\mathbf{R}}_{\beta\alpha}\, c^\dagger_{\mathbf{R}\beta}\,. \tag{11}$$

Instead of expressing the Gutzwiller projector in terms of the original basis as in Eq. (4) we adopt the following mixed *original-natural*[33] basis form

$$\mathcal{P}_{\mathbf{R}} = \sum_{\Gamma n} \lambda(\mathbf{R})_{\Gamma n}\,|\Gamma,\mathbf{R}\rangle\langle n,\mathbf{R}|, \tag{12}$$

where, by assumption, $|\Gamma,\mathbf{R}\rangle$ are Fock states in the original $c_{\mathbf{R}\alpha}$ basis, while $|n,\mathbf{R}\rangle$ are Fock states in the natural basis, namely in terms of the $d_{\mathbf{R}\alpha}$ operators. In other words, a generic state $|n,\mathbf{R}\rangle$ is identified by the occupation numbers $n_\beta(n,\mathbf{R}) \in \{0,1\}$—with $\beta \in \{1,\ldots,M\}$—and has the explicit expression

$$|n,\mathbf{R}\rangle = (d^\dagger_{\mathbf{R}1})^{n_1(n,\mathbf{R})} \ldots (d^\dagger_{\mathbf{R}M})^{n_M(n,\mathbf{R})}\,|0\rangle. \tag{13}$$

For later convenience we adopt the convention that the order of the $|\Gamma,\mathbf{R}\rangle$ and the $|n,\mathbf{R}\rangle$ states is the same. For instance, if the second Γ vector in Eq. (12) is $c^\dagger_{1\uparrow}c^\dagger_{2\downarrow}\,|0\rangle$, then the second n vector is $d^\dagger_{1\uparrow}d^\dagger_{2\downarrow}\,|0\rangle$.

B. The ϕ matrix

Let us introduce the uncorrelated occupation-probability matrix $P^0(\mathbf{R})$[32] with elements

$$[P^0(\mathbf{R})]_{nn'} \equiv \langle\Psi_0|\,|n',\mathbf{R}\rangle\langle n,\mathbf{R}|\,|\Psi_0\rangle = \delta_{nn'}\, P^0_n(\mathbf{R}), \tag{14}$$

where

$$P^0_n(\mathbf{R}) = \prod_{\beta=1}^{M} \left(n^0_{\mathbf{R}\beta}\right)^{n_\beta(n,\mathbf{R})}\left(1-n^0_{\mathbf{R}\beta}\right)^{1-n_\beta(n,\mathbf{R})}. \tag{15}$$

We note that $n^0_{\mathbf{R}\beta}$ are the elements of the diagonal density matrix of Eq. (9) and denote the occupation numbers of the natural states β. We also introduce the matrix representation of the operators $d_{\mathbf{R}\beta}$ and $c_{\mathbf{R}\beta}$,

$$d_{\mathbf{R}\beta} \to (d_{\mathbf{R}\beta})_{nn'} = \langle n,\mathbf{R}|d_{\mathbf{R}\beta}|n',\mathbf{R}\rangle \tag{16}$$

$$c_{\mathbf{R}\beta} \to (c_{\mathbf{R}\beta})_{\Gamma\Gamma'} = \langle\Gamma,\mathbf{R}|c_{\mathbf{R}\beta}|\Gamma',\mathbf{R}\rangle. \tag{17}$$

Notice that, if we respect the convention that the order of the $|\Gamma,\mathbf{R}\rangle$ and the $|n,\mathbf{R}\rangle$ states is the same, we have that

$$(c_{\mathbf{R}\beta})_{ij} = (d_{\mathbf{R}\beta})_{ij} \equiv (f_\beta)_{ij} \quad \forall\,\beta,i,j. \tag{18}$$

We now define the matrices $\lambda(\mathbf{R})$ and $U(\mathbf{R})$ with elements $\lambda_{\Gamma n}(\mathbf{R})$ [Eq. (12)] and $U_{\Gamma\Gamma'}(\mathbf{R})$ [Eq. (2)]. Notice that $\lambda(\mathbf{R})$ is defined in the original-natural and $U(\mathbf{R})$ is defined in the original-original basis. With the above definitions, the expectation value of any local observable can be calculated as

$$\langle\Psi_0|\,\mathcal{P}^\dagger\hat{\mathcal{O}}(\mathbf{R})\mathcal{P}\,\,|\Psi_0\rangle = \mathrm{Tr}\big(P^0(\mathbf{R})\lambda^\dagger(\mathbf{R})\,\mathcal{O}(\mathbf{R})\,\lambda(\mathbf{R})\big), \tag{19}$$

where

$$\mathcal{O}_{\Gamma\Gamma'}(\mathbf{R}) = \langle\Gamma|\hat{\mathcal{O}}|\Gamma'\rangle, \tag{20}$$

and the Gutzwiller constraints [Eqs. (5) and (6)] can be written as

$$\mathrm{Tr}(P^0(\mathbf{R})\lambda^\dagger(\mathbf{R})\lambda(\mathbf{R})) = 1 \tag{21}$$

$$\mathrm{Tr}(P^0(\mathbf{R})\lambda^\dagger(\mathbf{R})\lambda(\mathbf{R})f^\dagger_\alpha f_\beta) = \langle\Psi_0|\, d^\dagger_{\mathbf{R}\alpha}d_{\mathbf{R}\beta}\,|\Psi_0\rangle. \tag{22}$$

The formalism is further simplified by defining the matrix

$$\phi(\mathbf{R}) = \lambda(\mathbf{R})\sqrt{P^0(\mathbf{R})}\,, \tag{23}$$

that was introduced in Ref. 33. The expectation value of any local observable is given by

$$\langle\Psi_0|\,\mathcal{P}^\dagger\hat{\mathcal{O}}(\mathbf{R})\mathcal{P}\,\,|\Psi_0\rangle = \mathrm{Tr}(\phi(\mathbf{R})^\dagger\,\mathcal{O}(\mathbf{R})\,\phi(\mathbf{R})). \tag{24}$$

The Gutzwiller constraints take the form

$$\mathrm{Tr}(\phi^\dagger(\mathbf{R})\phi(\mathbf{R})) = 1, \tag{25}$$

$$\mathrm{Tr}(\phi^\dagger(\mathbf{R})\phi(\mathbf{R})\,f^\dagger_\alpha f_\beta) = \langle\Psi_0|\, d^\dagger_{\mathbf{R}\alpha}d_{\mathbf{R}\beta}\,|\Psi_0\rangle \equiv \delta_{\alpha\beta}\, n^0_{\mathbf{R}\alpha}, \tag{26}$$

and the variational energy [Eq. (7)] is, in the Gutzwiller approximation, given by[33]

$$\mathcal{E}_{\mathrm{var}} = \sum_{\mathbf{R}\mathbf{R}'}\sum_{\gamma\delta} \tilde{t}^{\gamma\delta}_{\mathbf{R}\mathbf{R}'}\,\langle\Psi_0|\, d^\dagger_{\mathbf{R},\gamma}d_{\mathbf{R}',\delta}\,|\Psi_0\rangle + \sum_{\mathbf{R}}\mathrm{Tr}(\phi(\mathbf{R})^\dagger\,U(\mathbf{R})\,\phi(\mathbf{R})), \tag{27}$$

where

$$\tilde{t}^{\gamma\delta}_{\mathbf{R}\mathbf{R}'} \equiv \sum_{\alpha\beta} t^{\alpha\beta}_{\mathbf{R}\mathbf{R}'}\,\mathcal{R}(\mathbf{R})_{\alpha\gamma}\mathcal{R}(\mathbf{R}')_{\beta\delta} \tag{28}$$

$$\mathcal{R}(\mathbf{R})_{\alpha\beta} = \frac{\mathrm{Tr}(\phi^\dagger(\mathbf{R})\,f^\dagger_\alpha\,\phi(\mathbf{R})\,f_\beta)}{\sqrt{n^0_\beta(\mathbf{R})\big[1-n^0_\beta(\mathbf{R})\big]}}. \tag{29}$$

In conclusion, within the formalism summarized in this section, the variational energy is a functional of $\phi(\mathbf{R})$ and $|\Psi_0\rangle$, to be minimized fulfilling the Gutzwiller constraints [Eqs. (25) and (26)].

C. Diagonal projector as a particular case

Let us assume that the coefficients of the matrix λ that define the projector $\mathcal{P}$ in Eq. (4) are diagonal,

$$\lambda(\mathbf{R})_{\Gamma\Gamma'} = \delta_{\Gamma\Gamma'}\,\lambda(\mathbf{R})_{\Gamma\Gamma}\,, \tag{30}$$

and that the *original* basis coincides with the *natural* basis,

$$\langle\Psi_0|\, c^\dagger_{\mathbf{R}\alpha}c_{\mathbf{R}\beta}\,|\Psi_0\rangle = \delta_{\alpha\beta}\,\langle\Psi_0|\, c^\dagger_{\mathbf{R}\alpha}c_{\mathbf{R}\alpha}\,|\Psi_0\rangle \equiv \langle\Psi_0|\, d^\dagger_{\mathbf{R}\alpha}d_{\mathbf{R}\beta}\,|\Psi_0\rangle. \tag{31}$$

From Eqs. (30) and (31) we have that

$$\phi(\mathbf{R})_{ij} = \delta_{ij}\,\phi(\mathbf{R})_{ii}, \tag{32}$$

and, consequently, the following equation hold for all local operators $\mathcal{O}(\mathbf{R})$

$$\mathrm{Tr}\,(\phi^\dagger(\mathbf{R})\,\phi(\mathbf{R})\,\mathcal{O}(\mathbf{R})) = \mathrm{Tr}(\phi^\dagger(\mathbf{R})\,\mathcal{O}(\mathbf{R})\,\phi(\mathbf{R})). \quad (33)$$

From Eq. (33) follows that the equations that characterize the Gutzwiller problem [Eqs. (25)–(29)] can be evaluated in terms of the variational parameters $\sqrt{m_\Gamma(\mathbf{R})}$ defined by Bünemann in Ref. 23

$$\phi(\mathbf{R})_{\Gamma\Gamma} = \sqrt{\langle\Psi_0|\,\mathcal{P}^\dagger|\Gamma,\mathbf{R}\rangle\langle\Gamma,\mathbf{R}|\mathcal{P}\;|\Psi_0\rangle} \equiv \sqrt{m_\Gamma(\mathbf{R})}. \quad (34)$$

A crucial observation in this work is that in the general case considered here, in which Eqs. (30) and (31) are not assumed, Eqs. (25)–(29) are expressed in terms of quadratic forms of the matrix elements of $\phi(\mathbf{R})$ instead of $\sqrt{m_\Gamma(\mathbf{R})}$, but in a formally identical way.

We conclude this section observing that the *physical* density matrix of the system

$$\rho_{\alpha\beta}(\mathbf{R}) \equiv \langle\Psi_0|\,\mathcal{P}^\dagger c^\dagger_{\mathbf{R}\alpha} c_{\mathbf{R}\beta}\mathcal{P}\;|\Psi_0\rangle = \mathrm{Tr}\,(\phi^\dagger(\mathbf{R})\,f^\dagger_\alpha f_\beta\,\phi(\mathbf{R})) \quad (35)$$

is *not* equal to the so-called *variational* density matrix

$$n^0_{\alpha\beta}(\mathbf{R}) \equiv \langle\Psi_0|\,d^\dagger_{\mathbf{R}\alpha} d_{\mathbf{R}\beta}\,|\Psi_0\rangle = \mathrm{Tr}(\phi^\dagger(\mathbf{R})\,\phi(\mathbf{R})\,f^\dagger_\alpha f_\beta) \quad (36)$$

when Eqs. (30)–(33) do not hold. In the general case the distinction between variational density matrix and physical density matrix needs to be taken into account.

IV. SYMMETRIES OF THE VARIATIONAL FUNCTION AND ϕ MATRIX

In this section we discuss in detail how to build symmetries in the Gutzwiller variational function. The site label $\mathbf{R}$ is dropped for simplicity. The procedure discussed here extends the method discussed in Ref. 34 to *general* point symmetry groups. The problem amounts to define the form of the ϕ matrix such that $|\Psi_G\rangle$ is invariant under the action of a matrix representation of a group G in the many-body $\mathbf{R}$-local space. The transformation law

$$\begin{aligned} g\,c^\dagger_\alpha\,g^{-1} &= \sum_\beta D_{\beta\alpha}(g)\,c^\dagger_\beta \quad \forall g \in G \\ g\,|0\rangle &= |0\rangle \end{aligned} \quad (37)$$

defines a representation[37] $R(G)$ of G in the local Hilbert space generated by the Fock configurations Γ, see Eq. (3),

$$g\,|\Gamma\rangle = \sum_{\Gamma'} R_{\Gamma'\Gamma}(g)\,|\Gamma'\rangle. \quad (38)$$

In the *original-original* basis [Eq. (4)] the invariance condition

$$g\,\mathcal{P}\,g^{-1} = \mathcal{P} \quad \forall g \in G \quad (39)$$

is equivalent to

$$[\lambda, R(g)] = 0 \quad \forall g \in G. \quad (40)$$

Let us *assume* that the most general transformation U that relates the original and the natural basis

$$\begin{aligned} d^\dagger_\alpha \equiv U\,c^\dagger_\alpha\,U^\dagger &= \sum_\beta \mathcal{U}_{\beta\alpha}\,c^\dagger_\beta \\ U\,|0\rangle &= |0\rangle \\ U\,|\Gamma\rangle &= |n\rangle, \end{aligned} \quad (41)$$

commutes with G, i.e., that

$$[U, R(g)] = [U^\dagger, R(g)] = 0 \quad \forall g \in G. \quad (42)$$

It can be shown, see Appendix A1, that Eq. (42) is verified for every group G whose elements do not mix configurations that belong to different eigenspaces of the number operator $\hat{N}$. This assumption is obviously verified by every geometry group, but excludes, for instance, the particle-hole transformation. A first consequence of Eq. (42) is that the matrix λ has the same form in the original-natural and in the original-original representation. In fact,

$$\mathcal{P} \equiv \sum_{\Gamma\Gamma'} \lambda_{\Gamma\Gamma'}|\Gamma\rangle\langle\Gamma'| = \sum_{\Gamma n} (\lambda U)_{\Gamma n}\,|\Gamma\rangle\langle n|, \quad (43)$$

and from Eqs. (40) and (42) we have that

$$[\lambda U, R(g)] = 0 \quad \forall g \in G. \quad (44)$$

Notice that from the assumed invariance of $|\Psi_0\rangle$ respect to G we have that, $\forall g \in G$,

$$\begin{aligned} P_{\Gamma\Gamma'} &\equiv \langle\Psi_0|\,|\Gamma'\rangle\langle\Gamma|\,|\Psi_0\rangle \\ &= \langle\Psi_0|\,|g\,\Gamma'\rangle\langle g\,\Gamma|\,|\Psi_0\rangle \\ &= (R^\dagger(g)\,P\,R(g))_{\Gamma\Gamma'}. \end{aligned} \quad (45)$$

Using Eq. (41) we can easily express P in terms of P^0 as follows

$$P = U\,P^0 U^\dagger, \quad (46)$$

where

$$P^0_{ij} \equiv \langle\Psi_0|\,|n_j\rangle\langle n_i|\,|\Psi_0\rangle, \quad (47)$$

so, combining Eqs. (45) and (46), we obtain that

$$P^0 = (U^\dagger R^\dagger(g) U) P^0 (U^\dagger R(g) U). \quad (48)$$

Equation (48) is equivalent, because of Eq. (42), to the following invariance relation for P^0:

$$[P^0, R(g)] = 0 \quad \forall g \in G. \quad (49)$$

From the above considerations and Eq. (23) we can conclude that ϕ satisfies the same invariance relation of the λ coefficients of the Gutzwiller projector in the original-original basis, i.e., that

$$[\phi, R(g)] = 0 \quad \forall g \in G. \quad (50)$$

In other words, we have proven that ϕ *has the same form of* λ expressed in the original-original Fock representation [Eq. (4)].

The set of all the ϕ matrices that satisfy Eq. (50) is a linear space $\mathcal{V}_\phi$. Consequently, there exists a basis of matrices $\{\phi_k\}$

such that

$$[\phi_k, R(g)] = 0 \quad \forall g \in G \tag{51}$$

$$\phi = \sum_k c_k \phi_k. \tag{52}$$

In this work we assume that c_k and ϕ_k are real. This means that $\mathcal{V}_\phi$ is a linear space over the field of *real* numbers. Notice that this does not restrict the variational freedom as long as the local interaction $\hat{H}_{\rm loc}$ is real. This excludes, for example, the spin-orbit coupling.

A. Calculation of $\{\phi_k\}$

In order to calculate $\{\phi_k\}$ it is convenient to apply a similarity transformation V to $R(G)$

$$R^V(g) = V R(g) V^\dagger \quad \forall g \in G \tag{53}$$

with the property to decompose $R(G)$ in irreducible representations.[37] More precisely, we need to calculate a unitary matrix V such that $R^V(G)$ is of the form

$$R^V(g) = \begin{pmatrix} R_1^V(g) & \cdots & 0 \\ \vdots & \ddots & \vdots \\ 0 & \cdots & R_s^V(g) \end{pmatrix} \quad \forall g \in G, \tag{54}$$

where (i) the representations $R_i^V(G)$ are irreducible for all $i \in \{1, \ldots, s\}$ and (ii) if two representations R_i^V, R_j^V are equivalent, then they are also equal. In Appendix A we derive a possible procedure to calculate explicitly the similarity transformation V utilized in this section for a general geometry group G.

Let us consider the linear space $\bar{\mathcal{V}}_\phi^V$ (over the *real* field) of the complex matrices $\bar{\phi}^V$ that satisfy the following equation:

$$[R^V(g), \bar{\phi}^V] = 0 \quad \forall g \in G. \tag{55}$$

It can be easily proven by means of the Schur lemma[37] that the most general $\bar{\phi}^V \in \bar{\mathcal{V}}_\phi^V$ is of the form

$$\bar{\phi}^V = \begin{pmatrix} p_1^V & \cdots & 0 \\ \vdots & \ddots & \vdots \\ 0 & \cdots & p_r^V \end{pmatrix}, \tag{56}$$

where the blocks $k \in \{1, \ldots, s\}$ correspond to inequivalent representations of G and each block is of the form

$$p_k^V = \begin{pmatrix} r_{11}\mathbb{1}_{d_k} & \cdots & r_{1n_k}\mathbb{1}_{d_k} \\ \vdots & \ddots & \vdots \\ r_{n_k1}\mathbb{1}_{d_k} & \cdots & r_{n_kn_k}\mathbb{1}_{d_k} \end{pmatrix}, \tag{57}$$

$\mathbb{1}_{d_k}$ being identity matrices of size $d_k \times d_k$, d_k being the dimension of each one of the irreducible equivalent representations of G repeated in the k-th block and r_{ij} being independent *complex* numbers. Equations (56) and (57) allow to define straightforwardly a basis $\{\bar{\phi}_k^V\}$ of $\bar{\mathcal{V}}_\phi^V$.

Let us define now the linear space of real matrices $\bar{\mathcal{V}}_\phi$ generated by the set of matrices $\{\bar{\phi}_k\}$ obtained as

$$\bar{\phi}_k \equiv V^\dagger \bar{\phi}_k^V V. \tag{58}$$

The linear space $\mathcal{V}_\phi$ that we need, see Eq. (50), is obtained as

$$\mathcal{V}_\phi = \bar{\mathcal{V}}_\phi \cap \mathcal{W}_\mathbb{R}, \tag{59}$$

where $\mathcal{W}_\mathbb{R}$ is the linear space of all *real* matrices. It is convenient, finally, to orthonormalize the basis set $\{\phi_k\}$ of $\mathcal{V}_\phi$ in order to have

$$\mathrm{Tr}(\phi_i^\dagger \phi_j) = \delta_{ij}. \tag{60}$$

B. Independent variational parameters

All the relevant quantities that define the variational energy, i.e., (i) the Gutzwiller constraints [Eqs. (25) and (26)], (ii) the $\mathcal{R}$ matrices [Eq. (29)], and (iii) the local-interaction energy [Eq. (27)], can be expressed in terms of quadratic forms in the c_k coefficients defined in Eq. (52) as follows:

$$\begin{aligned} \mathcal{R}_{\alpha\beta} &= \sum_{ij} c_i c_j \frac{\mathrm{Tr}(\phi_i^\dagger f_\alpha^\dagger \phi_j f_\beta)}{\sqrt{n_\beta^0(1-n_\beta^0)}} \\ &\equiv \sum_{ij} c_i c_j \frac{M_{\alpha\beta}^{ij}}{\sqrt{n_\beta^0(1-n_\beta^0)}} \\ &= \sum_{ij} c_i c_j \frac{1}{2} \frac{M_{\alpha\beta}^{ij} + M_{\alpha\beta}^{ji}}{\sqrt{n_\beta^0(1-n_\beta^0)}} \\ &\equiv \langle c| \frac{M_{\alpha\beta}^S}{\sqrt{n_\beta^0(1-n_\beta^0)}} |c\rangle, \end{aligned} \tag{61}$$

$$\begin{aligned} n_{\alpha\beta}^0 &\equiv \sum_{ij} c_i c_j \mathrm{Tr}(\phi_i^\dagger \phi_j \, f_\alpha^\dagger f_\beta) \\ &\equiv \sum_{ij} c_i c_j N_{\alpha\beta}^{ij} = \sum_{ij} c_i c_j \frac{1}{2}\left(N_{\alpha\beta}^{ij} + N_{\alpha\beta}^{ji}\right) \\ &\equiv \langle c| N_{\alpha\beta}^S |c\rangle, \end{aligned} \tag{62}$$

$$\begin{aligned} \langle \Psi_0| \mathcal{P}^\dagger \hat{H}_{\rm loc} \mathcal{P} |\Psi_0\rangle &= \sum_{ij} c_i c_j \mathrm{Tr}(\phi_i^\dagger U \phi_j) \\ &\equiv \sum_{ij} c_i c_j U^{ij} \equiv \langle c| U |c\rangle. \end{aligned} \tag{63}$$

Notice that the tensors M^S, N^S, and U are fully determined by the symmetry of the wave function [Eq. (1)] and the number of orbitals. For this reason, it is generally convenient to precalculate them before starting the numerical minimization of the variational energy. This point will be further discussed in Sec. VII D.

C. Simplified variational ansatz

The complexity of the numerical problem is considerably reduced if the mixing of different atomic configurations is neglected in the Gutzwiller projector. This amounts to assume that the matrix ϕ defined in Eq. (23) has the form

$$\phi = \sum_h c_k^{\rm int} \phi_h^{\rm int}, \tag{64}$$

$$\phi_h^{\rm int} \equiv P_h^{\rm int} / \sqrt{\mathrm{Tr}\left(\left[P_h^{\rm int}\right]^2\right)}, \tag{65}$$

where $P_h^{\rm int}$ are the orthogonal projectors onto the eigenspaces of the local atomic interaction $\hat{H}_{\rm int}$. Although the variational parameters neglected in Eqs. (64) and (65) can play a crucial role in some case,[33] this simplified ansatz merits mention for at least two reasons. (i) It still allows us to solve exactly the problem in the atomic limit and (ii) the number of independent variational parameters is generally extremely lower in this approximation, allowing us to perform calculations not feasible otherwise. Furthermore, once a variational result

$$\phi_0 \equiv \sum_h c_{0h}^{\rm int}\, \phi_h^{\rm int} \tag{66}$$

is obtained assuming Eqs. (64) and (65), it can be used as a good starting point c for the self-consistent search of the energy minimum with the more general variational space discussed before, see Eq. (52),

$$c_k = \mathrm{Tr}(\phi_k^\dagger \phi_0), \tag{67}$$

with the result to speed up the calculation. Notice, in fact, that $[\hat{H}_{\rm int}, G] = 0$, implying that

$$[\phi_0, R(g)] = 0 \quad \forall g \in G, \tag{68}$$

i.e., that $\phi_0 \in \mathcal{V}_\phi$.

V. NUMERICAL OPTIMIZATION OF THE VARIATIONAL ENERGY

In this section we discuss in detail the self-consistent numerical strategy to minimize the energy [Eq. (27)] fulfilling the Gutzwiller constraints [Eqs. (25) and (26)].

Notice that the formulation of the Gutzwiller problem through Eqs. (25)–(27) is formally analog to the constrained formulation of DFT derived by Levy[38,39] and Lieb.[40] In fact, the variational energy can be expressed as a functional of the *variational* density matrix n^0, see Eq. (36),

$$\mathcal{E}_{\rm var}[n^0] = \min_{n^0} \mathcal{E}_{\rm var}\,[c, \Psi_0]\,, \tag{69}$$

where $\min_{n^0}$ denotes the minimum over the set of variational parameters c and $|\Psi_0\rangle$, satisfying the Gutzwiller constraints [Eqs. (25) and (26)] at fixed n^0. In this work the Gutzwiller problem is solved by calculating the density functional $\mathcal{E}_{\rm var}[n^0]$ and minimizing it with respect to n^0.

For clarity reasons we have structured the rest of this section as an exposition of the numerical procedure, omitting the mathematical proofs. The mathematical details can be found in the Appendices.

A. Preliminary calculation

Let us consider the Gutzwiller renormalized nonlocal tight-binding operator

$$\hat{T}^G = \sum_{\alpha\beta} \sum_{\mathbf{R}\neq\mathbf{R}'} \tilde{t}_{\mathbf{R}\mathbf{R}'}^{\alpha\beta}\, d_{\mathbf{R}\alpha}^\dagger d_{\mathbf{R}'\beta}, \tag{70}$$

where

$$\tilde{t}_{\mathbf{R}\mathbf{R}'}^{\gamma\delta} \equiv \sum_{\alpha\beta} t_{\mathbf{R}\mathbf{R}'}^{\alpha\beta}\, \mathcal{R}_{\alpha\gamma} \mathcal{R}_{\beta\delta}. \tag{71}$$

For later convenience, we consider a general one-body Hamiltonian

$$\hat{H}^G = \hat{T}^G + \Delta\hat{H} = \sum_{\mathbf{k}n} \epsilon_{\mathbf{k}n}^G\, \eta_{\mathbf{k}n}^\dagger \eta_{\mathbf{k}n}, \tag{72}$$

where $\Delta\hat{H}$ is a given local operator.

Let $|\Psi_0\rangle$ be the ground state of $\hat{H}^G$. It can be easily verified that

$$\frac{\partial \langle\Psi_0|\, \hat{T}^G[\mathcal{R}]\, |\Psi_0\rangle}{\partial \mathcal{R}_{\alpha\beta}} = 2 \sum_{\mathbf{k}} [t_{\mathbf{k}} \mathcal{R}\, U_{\mathbf{k}} f_{\mathbf{k}} U_{\mathbf{k}}^\dagger]_{\alpha\beta}, \tag{73}$$

where

$$(f_{\mathbf{k}})_{nm} = \theta\left(-\epsilon_{\mathbf{k}n}^G\right) \delta_{nm}, \tag{74}$$

$$\eta_{\mathbf{k}n}^\dagger = \sum_i (U_{\mathbf{k}})_{\alpha n}\, d_{\mathbf{k}\alpha}^\dagger\,. \tag{75}$$

Equation (73) will be used in the following subsections, where two important inner parts of our numerical scheme are described in detail.

B. Slater determinant optimization step

For later convenience, in this section we solve the problem of calculating the state $|\Psi_0\rangle$ that realizes the minimum of the Gutzwiller variational energy at fixed c

$$\begin{aligned} \mathcal{E}_{n^0,\mathcal{R}} &= \min_{|\Psi\rangle \in S_{n^0}} \langle\Psi|\, \hat{T}^G\, |\Psi\rangle \\ S_{n^0} &\equiv \left\{ |\Psi\rangle \text{ t.c. } \langle\Psi|\, d_{\mathbf{R}\alpha}^\dagger d_{\mathbf{R}\beta}\, |\Psi\rangle = \delta_{\alpha\beta} n_\alpha^0 \right\}, \end{aligned} \tag{76}$$

where $\hat{T}^G$ is given by Eqs. (70) and (71). Note that the functional $\mathcal{E}_{n^0,\mathcal{R}}$ depends on c only indirectly through $\mathcal{R}$, which is given by

$$\mathcal{R}_{\alpha\beta} = \frac{\langle c|\, M_{\alpha\beta}^S\, |c\rangle}{\sqrt{n_\beta^0 (1 - n_\beta^0)}}; \tag{77}$$

see Eqs. (29) and (61).

It is convenient to account for the Gutzwiller constraints employing the Lagrange multipliers method. We introduce

$$\hat{H}^G[\mathcal{R}, \lambda] = \hat{T}^G + \Delta\hat{H}, \tag{78}$$

where

$$\Delta\hat{H} = \sum_{\mathbf{R}} \sum_{\alpha\beta} \lambda_{\alpha\beta}\, d_{\mathbf{R}\alpha}^\dagger d_{\mathbf{R}\beta}. \tag{79}$$

Notice that $\hat{H}^G$ has the same form of Eq. (72). Finally, we calculate the ground state $|\Psi_0\rangle$ of $\hat{H}^G[\mathcal{R}, \lambda]$ for $\lambda_{\alpha\beta}$ such that the Gutzwiller constraints [Eqs. (25) and (26)] are satisfied. Once the Lagrange multipliers $\lambda_{\alpha\beta}$ are known we compute Eq. (73).

In summary, the calculations described in this section associate the input variables n_β^0 and $\mathcal{R}_{\alpha\beta}$ to the output matrix

$$\mathcal{D}_{\alpha\beta} \equiv \frac{\partial \langle\Psi_0|\, \hat{T}^G\, |\Psi_0\rangle}{\partial \mathcal{R}_{\alpha\beta}}; \tag{80}$$

see Fig. 1.

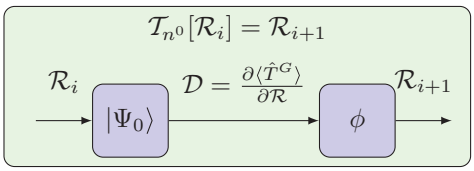

FIG. 1. (Color online) Flow chart representing the numerical calculation of the functional $\mathcal{T}_{n^0}$.

C. ϕ-matrix optimization step

In this section we derive the numerical procedure to minimize the Gutzwiller energy functional

$$\mathcal{E}_{\Psi_0}[c] = \langle \Psi_0 | \hat{T}^G | \Psi_0 \rangle + \langle c | U | c \rangle, \tag{81}$$

where $\hat{T}^G$ is given by Eqs. (70) and (71) and $\mathcal{R}$ depends on c through Eq. (77), keeping the Slater determinant $|\Psi_0\rangle$ fixed and respecting the Gutzwiller constraints

$$\langle c|c\rangle = 1, \tag{82}$$

$$\langle c| N^S_{\alpha\beta} |c\rangle = \delta_{\alpha\beta}\, n^0_\alpha. \tag{83}$$

In order to solve this problem we adopt the following linearization procedure, which is based on Appendix B. We consider the Hermitian matrix

$$F[\mathcal{D},\lambda] = H[\mathcal{D}] + L[\lambda], \tag{84}$$

where $\mathcal{D}_{\alpha\beta}$ is defined by Eq. (80), and

$$H[\mathcal{D}] = U + \sum_{\alpha\beta} \mathcal{D}_{\alpha\beta} \frac{M^S_{\alpha\beta}}{\sqrt{n^0_\beta (1 - n^0_\beta)}}, \tag{85}$$

$$L[\lambda] = \sum_{\alpha\beta} \lambda_{\alpha\beta}\, N^S_{\alpha\beta}. \tag{86}$$

We then calculate the ground state c of $F[\mathcal{D},\lambda]$ for λ such that the Gutzwiller constraints [Eqs. (82) and (83)] are satisfied. The obtained vector c is used to define a new $\mathcal{R}$ through Eq. (77).

Notice that the matrix $\mathcal{D}_{\alpha\beta}$ entirely encodes the dependency of the problem on $|\Psi_0\rangle$ in Eq. (84). In summary, the above calculations associate to the input variables n^0_β and $\mathcal{D}_{\alpha\beta}$ the output renormalizaton matrix $\mathcal{R}_{\alpha\beta}$; see Fig. 1.

D. Fixed-point formulation

A very important observation in our implementation is that the composition of the two optimization steps derived in Secs. V B and V C can be described as a functional $\mathcal{T}_{n^0}$ that associates a given renormalization matrix $\mathcal{R}_i$ to a new renormalization matrix $\mathcal{R}_{i+1}$

$$\mathcal{R}_{i+1} = \mathcal{T}_{n^0}[\mathcal{R}_i]; \tag{87}$$

see Fig. 1. This operation lead to a reduction of the variational energy unless, by definition, $\mathcal{R}$ solves the equation

$$\mathcal{T}_{n^0}[\mathcal{R}] - \mathcal{R} = 0. \tag{88}$$

In this case, $\mathcal{R}$ defines a stationary point of the energy functional. This observation results in a formulation of the minimization of the variational energy at fixed n^0 as a *fixpoint problem*, that can be solved in several ways.[41] A first possibility is to use $\mathcal{R}_i$ as an input to obtain $\mathcal{R}_{i+1}$ and iterate the procedure up to convergence. This procedure is commonly referred to as *forward recursion* method.[6,42] However, as it will be shown in Sec. VII D, the application of the *Newton method* is generally much more efficient.

We underline that the size of $\mathcal{R}$ is equal to the number of orbitals and that the number of independent parameters that define it is often reduced by symmetry. For this reason the solution of Eq. (88) generally requires a few Newton steps to converge; see Sec. VII D. The problem of the exponential scaling of the local many-body space affects the numerical algorithm exclusively through the solution for the ground state of $F[\mathcal{D},\lambda]$; see Eq. (84). The size of the matrix $F[\mathcal{D},\lambda]$ is, in fact, equal to the dimension of the vector c. Nevertheless, the calculation of the ground state of $F[\mathcal{D},\lambda]$ is not numerically problematic for two reasons. (i) The dimension of c is reduced by symmetries, as will be shown in Sec. VII D. (ii) The calculation of the ground state of $F[\mathcal{D},\lambda]$ does not require a full diagonalization. Less computationally demanding algorithms, such as the power method or the Lanczos method, can be employed. See Sec. VII D for further details.

We remark that the self-consistent numerical algorithm derived in this paper requires, as a starting point, only a initial "guess" for the variational density matrix n^0 and the matrix $\mathcal{R}$. It is not necessary to construct a good initial guess for the whole Gutzwiller wave function, i.e., for the matrix ϕ, while this would be necessary in order to perform a direct constrained minimization of the energy functional [Eq. (27)]. This implies that the stability of the algorithm is not affected by the exponential scaling of the number of parameters involved in the calculation. This point will be further discussed in Sec. VII D.

VI. APPLICATION TO LDA + GUTZWILLER

In this section we briefly discuss how to combine the Gutzwiller scheme with a first-principles calculation of the uncorrelated electron structure as an input, applying the DFT scheme with LDA. This combined scheme is named LDA + G. We also outline how the Gutzwiller solver has to be modified in order to account for the double counting.[21] The double counting appears as a mean-field contribution in the exchange-correlation taken into account in the LDA calculation.

As a starting point we consider the Kohn-Sham reference system obtained within a converged LDA calculation

$$\hat{H}_{\mathrm{LDA}} = \sum_{\mathbf{k}} \sum_{n} \epsilon^{\mathrm{KS}}_{\mathbf{k}n}\, \eta^\dagger_{\mathbf{k}n} \eta_{\mathbf{k}n}, \tag{89}$$

$$\eta^\dagger_{\mathbf{k}n} |0\rangle \equiv \left| \psi^{\mathrm{KS}}_{\mathbf{k}n} \right\rangle. \tag{90}$$

In order to be able to apply LDA + G the tight-binding Hamiltonian [Eq. (89)] must, first, be expressed in terms of a proper localized basis set[20] $|\chi_{k\alpha}\rangle$, where α labels both spin σ and orbital a. This can be done by means of the overlap matrix

$$[S_{\mathbf{k}}]_{n\alpha} = \left\langle \psi^{\mathrm{KS}}_{\mathbf{k}n} \middle| \chi_{\mathbf{k}\alpha} \right\rangle, \tag{91}$$

giving

$$\hat{H}_{\rm LDA} = \sum_{\mathbf{k}} \sum_{\alpha\beta} \epsilon_{\mathbf{k}}^{\alpha\beta} \, c_{\mathbf{k}\alpha}^{\dagger} c_{\mathbf{k}\beta}, \tag{92}$$

$$\epsilon_{\mathbf{k}}^{\alpha\beta} = \sum_{n} [S_{\mathbf{k}}^{\dagger}]_{\alpha n} \, \epsilon_{\mathbf{k}n}^{\rm KS} \, [S_{\mathbf{k}}]_{n\beta}, \tag{93}$$

$$c_{\mathbf{k}\alpha}^{\dagger}|0\rangle \equiv |\chi_{k\alpha}\rangle. \tag{94}$$

In order to express $\hat{H}_{\rm LDA}$ in the same form of Eq. (2) we separate $\hat{H}_{\rm LDA}$ in a nonlocal part $\hat{T}$ and in a local part (the crystal fields) as follows:

$$\hat{H}_{\rm LDA} = \hat{T} + \hat{L}, \tag{95}$$

$$\hat{T} = \sum_{\mathbf{k}} \sum_{\alpha\beta} t_{\mathbf{k}}^{\alpha\beta} \, c_{\mathbf{k}\alpha}^{\dagger} c_{\mathbf{k}\beta}, \tag{96}$$

$$\hat{L} = \sum_{\mathbf{R}} \sum_{\alpha\beta} l^{\alpha\beta} \, c_{\mathbf{R}\alpha}^{\dagger} c_{\mathbf{R}\beta}, \tag{97}$$

where

$$l^{\alpha\beta} = \frac{1}{\Omega} \sum_{\mathbf{k}} \epsilon_{\mathbf{k}}^{\alpha\beta}, \tag{98}$$

$$t_{\mathbf{k}}^{\alpha\beta} = \epsilon_{\mathbf{k}}^{\alpha\beta} - l^{\alpha\beta}, \tag{99}$$

and Ω is the number of sites $\mathbf{R}$. The on-site electron interaction can be modeled by the Slater-Kanamori rotationally invariant atomic interaction[24]

$$\hat{H}_{\rm int} = \sum_{\mathbf{R}} \hat{H}_{\rm int}^{\mathbf{R}}, \tag{100}$$

$$\begin{aligned} \hat{H}_{\rm int}^{\mathbf{R}} = {} & U \sum_{a} \hat{n}_{\mathbf{R}a\uparrow} \hat{n}_{\mathbf{R}a\downarrow} + \frac{U'}{2} \sum_{a\neq b} \sum_{\sigma\sigma'} \hat{n}_{\mathbf{R}a\sigma} \hat{n}_{\mathbf{R}b\sigma'} \\ & - \frac{J}{2} \sum_{a\neq b} \sum_{\sigma} c_{\mathbf{R}a\sigma}^{\dagger} c_{\mathbf{R}a-\sigma} c_{\mathbf{R}b-\sigma}^{\dagger} c_{\mathbf{R}b\sigma} \\ & - \frac{J'}{2} \sum_{a\neq b} c_{\mathbf{R}a\uparrow}^{\dagger} c_{\mathbf{R}a\downarrow}^{\dagger} c_{\mathbf{R}b\uparrow} c_{\mathbf{R}b\downarrow}. \end{aligned} \tag{101}$$

We underline that the form [Eq. (101)] for $\hat{H}_{\rm int}$ is obtained by implicitly assuming that the single-particle basis $|\chi_{k\alpha}\rangle$ is given by *real* orbitals, i.e., the cubic (crystal) harmonics. It can be proven that the condition $U = U' + J + J'$ ensures the rotational invariance in the orbital space. The additional condition $J = J'$ can be assumed whenever the spin-orbital coupling is negligible.[20]

Our model is now defined in the form of Eq. (2), with $\hat{T}$ given by Eq. (96) and $\hat{H}_{\rm loc} = \hat{H}_{\rm int} + \hat{L}$. An additional on-site term, the double counting, needs to be added to Eq. (27) as the average orbital-independent interaction energy is already included in LDA. A common choice of the double counting term is[21,22]

$$E_{\rm dc}[\rho] = \frac{\bar{U}}{2} n(n-1) - \sum_{\sigma} \frac{\bar{J}}{2} n_{\sigma}(n_{\sigma} - 1), \tag{102}$$

$$\begin{aligned} \bar{U} &= \frac{U + 2lJ}{2l+1}, \\ \bar{J} &= \bar{U} - U' + J, \end{aligned} \tag{103}$$

where l is the angular-momentum quantum number of the considered localized basis set,

$$\begin{aligned} n &\equiv \sum_{\sigma} n_{\sigma} \equiv \sum_{a\sigma} n_{a\sigma}, \\ n_{\alpha} &\equiv \rho_{\alpha\alpha}, \end{aligned} \tag{104}$$

see Eq. (35), and n_{α} is the mean value of $c_{\mathbf{R}\alpha}^{\dagger} c_{\mathbf{R}\alpha}$ with respect to the Gutzwiller wave function, which is given by

$$\begin{aligned} n_{\alpha} &= \sum_{ij} c_i c_j {\rm Tr}(\phi_i^{\dagger} \, f_{\alpha}^{\dagger} f_{\alpha} \, \phi_j), \\ &\equiv \sum_{ij} c_i c_j \, P_{\alpha\alpha}^{ij} \equiv \langle c| \, P_{\alpha\alpha} \, |c\rangle. \end{aligned} \tag{105}$$

The presence of the double counting term gives rise to the following additional term in Eq. (84):

$$D[c] = \sum_{\alpha} \frac{\partial E_{\rm dc}}{\partial n_{\alpha}} P_{\alpha\alpha}. \tag{106}$$

When the self-consistent Gutzwiller calculation is converged the result can be fed back to the LDA code. By calculating the density matrix

$$[\rho_{\mathbf{k}}]_{\alpha\beta} \equiv \langle \Psi_0| \, \mathcal{P}^{\dagger} c_{k\alpha}^{\dagger} c_{k\beta} \mathcal{P} \, \, |\Psi_0\rangle \tag{107}$$

and representing it in the Kohn-Sham basis

$$\left[\rho_{\mathbf{k}}^{\rm KS}\right]_{nm} = \sum_{\alpha\beta} [S_{\mathbf{k}}]_{n\alpha} \, [\rho_{\mathbf{k}}]_{\alpha\beta} \, [S_{\mathbf{k}}^{\dagger}]_{m\beta}, \tag{108}$$

it is possible to get a prescription how to transform the Kohn-Sham eigenfunctions and occupancies in order to reproduce the physical Gutzwiller electron density.[20] To the new total density corresponds a new effective potential for the Kohn-Sham reference system that, in turn, defines a new tight-binding Hamiltonian.

The procedure is iterated until self-consistency is reached.

VII. RESULTS

This section has two purposes. (i) As a proof of concept we present some numerical result in comparison with other calculations based on different methods. (ii) We outline several technical details of the calculations and the speed of convergence of the algorithm.

Test calculations have been performed on multiorbital model Hamiltonians of the form

$$\hat{H} = \sum_{\mathbf{k}\sigma} \sum_{ab} t_{\mathbf{k}}^{ab} c_{\mathbf{k}a\sigma}^{\dagger} c_{\mathbf{k}b\sigma} + \sum_{\mathbf{R}\sigma} \sum_{ab} l^{ab} \, c_{\mathbf{R}a\sigma}^{\dagger} c_{\mathbf{R}b\sigma} + \hat{H}_{\rm int}, \tag{109}$$

where the structure of $\hat{H}_{\rm int}$ was defined in Eq. (101). A paramagnetic Gutzwiller wave function has been assumed in all the calculations shown in this section. The hopping matrix has been set up as either (i) nearest-neighbor hopping on a three-dimensional cubic lattice, giving a noninteracting DOS with cusps close to half the bandwidth, or (ii) nearest-neighbor hopping on a Bethe graph with infinite coordination number, corresponding to a semicircular noninteracting DOS. In both cases the half bandwidth W is set as the unit of energy.

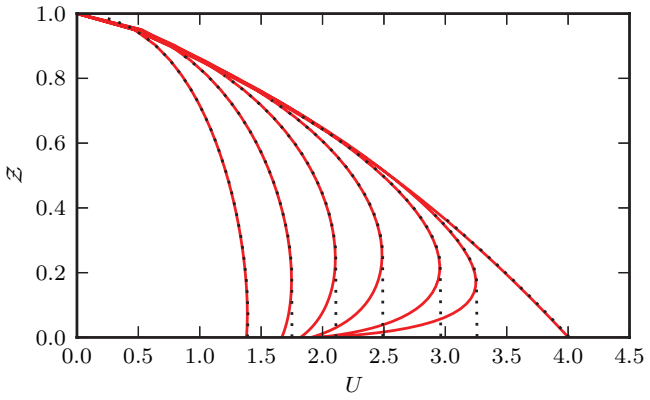

FIG. 2. (Color online) Comparison of results for two degenerate bands on the 3D cubic lattice with rotational-invariant Hunds interaction, from Gutzwiller (solid lines) and slave-boson[43] (dotted lines), showing the quasiparticle weight $\mathcal{Z}$ as a function of U and (from right to left), $J/U = 0$, 0.01, 0.02, 0.05, 0.10, 0.20, 0.45. Additionally, the higher energy fixpoint solutions of Eq. (88) at finite J/U are reported.

A. Two-bands Hubbard model

First, let us consider the case of two orbitals. In the special case of half-filling and degenerate bands we compare our calculations with the available results obtained from Ref. 43 by means of the rotationally invariant slave-boson technique,[43–47] which is equivalent to the Gutzwiller variational method on the mean field level.[48,49] In this case $t_{\mathbf{k}}^{ab}$ is set up as nearest-neighbor hopping on a three-dimensional cubic lattice

$$t_{\mathbf{k}}^{ab} = -\,t_{ab}^{0}\,\frac{1}{3}\sum_{\mu=1}^{3}\cos(k_\mu), \tag{110}$$

with $t_{ab}^{0} = \delta_{ab}$. For this specific model, in which the single-particle energy dispersion of the two bands are identical, we have that

$$\mathcal{R}_{ab} = \sqrt{\mathcal{Z}}\,\delta_{ab}, \tag{111}$$

where $\mathcal{Z}$ can be interpreted as a measure of the quasiparticle renormalization weight.[50] As shown in Fig. 2, the Gutzwiller calculation gives the same values of $\mathcal{Z}$ as a function of U and J/U as the slave-boson calculations. The Brinkman-Rice transition[11] occurs at a strongly J-dependent critical U. This well-known fact[51] supports the argument that the spin-exchange on-site interaction needs to be taken into account to accurately describe strongly correlated systems. Furthermore, while for $J/U = 0$ the phase transition is second order, at finite J/U it becomes first order, with a hysteresis region characterized by an additional fixpoint solution of Eq. (88), corresponding to a second stationary point of the variational energy; see Fig. 2. To our knowledge this solution has never been reported before in either the Gutzwiller or in the slave-boson approximation.

Let us consider the more general case of nondegenerate bands with finite crystal field splitting Δ,

$$\sum_{ab} l^{ab}\, c_{\mathbf{R}a\sigma}^{\dagger} c_{\mathbf{R}b\sigma} = \Delta\,(\hat{n}_{\mathbf{R}1\sigma} - \hat{n}_{\mathbf{R}2\sigma}). \tag{112}$$

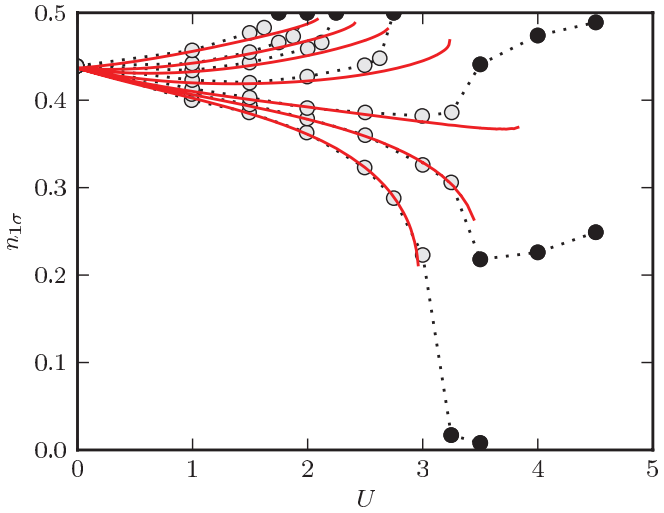

FIG. 3. (Color online) Filling per spin of orbital 1 for $\Delta = 0.2$ and different values of J/U. From bottom to top, $J/U =$ 0,0.01,0.02,0.05,0.1,0.15,0.25. The continue lines correspond to our Gutzwiller results for the metallic phase at half-filling. Open (full) symbols correspond to metallic (insulating) solutions obtained from DMFT[52] at inverse temperature $\beta = 25$.

This model has been studied in detail with DMFT in Ref. 52. Here we compare our Gutzwiller results with part of the available DMFT data. This gives an opportunity to discuss some features of the specific implementation derived in this work and to introduce some general merits and limits of the Gutzwiller variational method in itself.

In Fig. 3 the expectation value of the filling per spin $\hat{n}_{1\sigma}$ is shown for several values of U and J/U. Following Sec. III, the expectation value of $\hat{n}_{1\sigma}$ is given by

$$n_{1\sigma} = \mathrm{Tr}(\phi^{\dagger}\, f_{1\sigma}^{\dagger} f_{1\sigma}\, \phi); \tag{113}$$

see Eq. (24). In the same figure the DMFT results from Ref. 52 are also shown. These calculations were performed assuming a semicircular density of states.

For the specific crystal field splitting considered, $\Delta = 0.2$, the system is metallic at small U and is driven toward a Mott insulating or an orbitally polarized phase, depending on the value of J/U, on increasing the interaction strength U. Notice that the DMFT and the Gutzwiller results are in very good agreement in the metallic phase, especially away from the Mott transition. This confirms that the quality of the Gutzwiller calculations is generally comparable with the quality of DMFT for the ground-state properties of strongly correlated metals.[20] On the contrary, the Mott-insulating phase cannot be described correctly by means of a Gutzwiller approximation. Nevertheless, it is correct to assume that $\mathcal{Z}$ approaching 0 indicates that the metallic phase becomes unstable, compatibly with the Brinkman-Rice scenario.[11] Notice that the critical coupling $U_c(J)$ of the Mott transition predicted by the Gutzwiller approximation is not accurate in general. For instance, at $J = 0$ the Gutzwiller calculation gives $U_c \approx 5$ for the semicircular density of states, which differs from the DMFT result,[52] $U_c^{\mathrm{DMFT}} \approx 4$ by 20% (not shown). Notice that the results of Fig. 2 were obtained assuming a

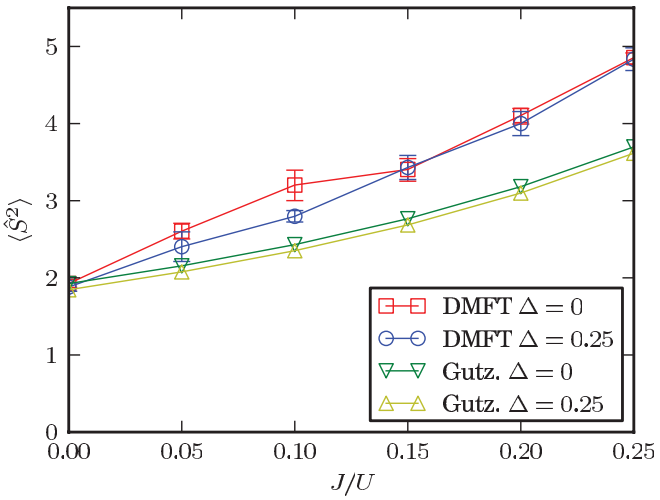

FIG. 4. (Color online) Gutzwiller expectation value of $\hat{S}^2$ for different values of J/U and crystal field splittings Δ, the total filling is six electrons per site and $U = 1$. Comparison with DMFT data at inverse temperature $\beta = 25$ from Ref. 53.

three-dimensional cubic lattice and not a semicircular density of states.

B. Five-band Hubbard model

In this section we study the Hamiltonian of the form [Eq. (109)] for five bands, describing correlated d electrons in a cubic crystal. We assume a semicircular density of states and that the full rotational symmetry is broken by a finite crystal field splitting Δ between the three t_{2g} and the two e_g orbitals, i.e.,

$$\sum_{ab} l^{ab} c^{\dagger}_{\mathbf{R}a\sigma} c_{\mathbf{R}b\sigma} = \Delta \sum_{a \in t_{2g}} \hat{n}_{\mathbf{R}a\sigma}. \tag{114}$$

This model has previously been used as a benchmark system in DMFT.[53] In our calculation we assume a paramagnetic Gutzwiller wave function invariant with respect to the symmetry point group of the cube. This allows us to reduce considerably the number of variational parameters; see Sec. VII D.

Let us consider the expectation value S^2 of the total spin squared $\hat{S}^2$, for which DMFT data are available in Ref. 53. From Eq. (24) we have that

$$S^2 = \mathrm{Tr}(\phi^{\dagger} \mathbf{S}^2 \phi), \tag{115}$$

where

$$\mathbf{S}_k = \sum_{a} \sum_{\sigma\sigma'} f^{\dagger}_{a\sigma} \frac{\sigma^k_{\sigma\sigma'}}{2} f_{a\sigma'} \tag{116}$$

and σ^k are the Pauli matrices. In Fig. 4 the behavior of S^2 is shown at fixed $U = 1$ for six electrons per site and several values of J/U. In the figure our results are compared with the DMFT data from Ref. 53. Consistently with DMFT, we find that S^2 grows monotonically on increasing J/U and that the crystal field splitting $\Delta = 0.25$ slightly reduces S^2 compared to the case of degenerate bands. Notice that the discrepancy between the Gutzwiller results and the DMFT data becomes larger on increasing J/U at fixed U. A similar qualitative behavior could be observed even in the calculation shown in Fig. 2 for the two-bands model. Nevertheless, the observed deviation between the Gutzwiller results and the DMFT data seems to be more substantial in this case.

C. Bilayer Hubbard model

In both the models previously considered the renormalization matrix $\mathcal{R}$ was diagonal due to symmetry. For completeness, we also consider the bilayer Hubbard model,[32,34,43] in which $\mathcal{R}$ have finite off-diagonal elements. In particular, we consider the Hamiltonian given by Eq. (109), assuming that the local hybridization term described by the matrix

$$l = \begin{pmatrix} 0 & V \\ V & 0 \end{pmatrix} \tag{117}$$

with $V = 0.25$, and a hopping matrix $t^{ab}_{\mathbf{k}}$ given by Eq. (110) as in Sec. VII A. Finally, we assume that the local interaction $\hat{H}_{\mathrm{int}}$ is given by Eq. (101) with $U' = J' = J = 0$. This model has previously been studied—with the same parameters—in Ref. 43 with the slave-boson method.

When the bandwidths are equal for the two bands (as in the present case) the matrix l defined in Eq. (117) can be diagonalized without modifying the hopping matrix $t^{ab}_{\mathbf{k}}$ for any $\mathbf{k}$.[43] This change of basis transforms the hybridization term l in a crystal field splitting between the bonding (+) and antibonding (−) orbitals. In the new basis both the effective renormalization matrix $\mathcal{Z}^0 \equiv [\mathcal{R}^0]^2$ and the density matrix are diagonal

$$\mathcal{Z}^0 = \begin{pmatrix} \mathcal{Z}_+ & 0 \\ 0 & \mathcal{Z}_- \end{pmatrix}, \quad n^0 = \begin{pmatrix} n_+ & 0 \\ 0 & n_- \end{pmatrix}, \tag{118}$$

and the coefficients $\mathcal{Z}_+, \mathcal{Z}_-$ can be interpreted as the quasiparticle renormalization weights of the bonding and antibonding orbitals, respectively. In the original basis, instead, $\mathcal{R}$ has nonzero off-diagonal elements and $\mathcal{Z} \equiv \mathcal{R}^2$ has the form $\mathcal{Z}_{11} = \mathcal{Z}_{22}$ and $\mathcal{Z}_{12} = \mathcal{Z}_{21}$, where

$$\mathcal{Z}_{11} = \frac{\mathcal{Z}_+ + \mathcal{Z}_-}{2} \tag{119}$$

$$|\mathcal{Z}_{12}| = \frac{|\mathcal{Z}_+ - \mathcal{Z}_-|}{2}. \tag{120}$$

In order to compare with the slave-boson results of Ref. 43 we have studied the system for $N = 1.88$ electrons per site. As seen in Fig. 5, the average of $\mathcal{Z}_+$ and $\mathcal{Z}_-$, given by $\mathcal{Z}_{11}$, decreases monotonically as a function of U as expected. Concomitantly, the difference between $\mathcal{Z}_+$ and $\mathcal{Z}_-$, given by $|\mathcal{Z}_{12}|$, progressively increases with U. Our calculations compare well with the slave-boson results, although we find a slightly lower renormalization of the antibonding state at large interactions.

D. Technical remarks

In this section we point out several technical details of the numerical simulations performed to derive the results presented above.

The main technical problem of the Gutzwiller method is that the dimension of c, see Eq. (52), scales exponentially with the number of correlated orbitals. Fortunately, this number can be highly reduced by taking into account the symmetries of

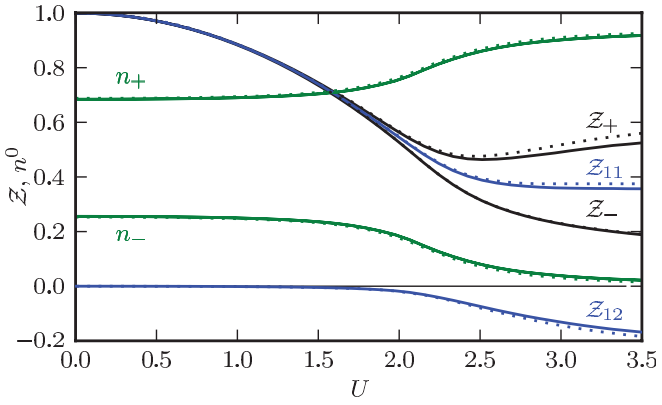

FIG. 5. (Color online) Gutzwiller renormalization matrix $\mathcal{Z}$ and filling of the bonding-antibonding bands for the two-bands bilayer Hubbard model with equal bandwidths, local hybridization $V = 0.25$, $U' = J' = J = 0$, and filling $N = 1.88$ (solid lines). Comparison with slave-boson results from Ref. 43 (dotted lines).

the system. As an example, the number of matrix elements of ϕ (i.e., the dimension squared of the local Fock space) is compared in Table I with the dimension of the vector c in the case of a paramagnetic Gutzwiller wave function invariant with respect to the point symmetry group of the cube. This simplification is very important, as $\dim(c)$ is equal to the size of $F[\mathcal{D},\lambda]$, see Eq. (84), whose ground state needs to be evaluated many times during the calculations. To compute the ground state of $F[\mathcal{D},\lambda]$, i.e., its eigenvector with the lowest eigenvalue, we have used the iterative Arnoldi based solver provided by the ARPACK library. This calculation is further speeded up by exploiting the sparsity of $F[\mathcal{D},\lambda]$, effectively reducing the cost of the necessary matrix-vector multiplications.

As anticipated in Sec. IV B, it is generally convenient to precalculate ϕ_k and the tensors $M^{ij}_{\alpha\beta}$, $N^{ij}_{\alpha\beta}$, and U^{ij} in order to further speed up the calculations. This reduces the construction of the matrix F to the sums in Eqs. (85) and (86) but increases the memory requirements. In fact, the total number of elements N_T in the tensors scales as

$$N_T = \left(2N_{\mathrm{orb}}^2 + 1\right)N_c^2 + N_c N_\Gamma^2 , \tag{121}$$

where N_c is the dimension of the vector c, N_{orb} is the number of orbitals, and $N_\Gamma = 2^{2N_{\mathrm{orb}}}$ is the dimension of the local space. However, the number of stored matrix elements can considerably reduced by exploiting the sparsity of the tensors. For instance, the number of nonzero elements in the tensors was reduced by around three orders of magnitude for the five-band Hubbard model of Sec. VII B. Eventually, in more

TABLE I. Dimensions of the variational space for one, three, and five atomic orbitals (corresponding to s, p, and d electrons). The number of matrix elements of ϕ, $2^{4N_{\mathrm{orb}}}$, is compared with the dimension of the vector c, which is reduced by the point group symmetry of the cubic lattice.

	l	N_{orb}	$2^{4N_{\mathrm{orb}}}$	$\dim(c)$
s	0	1	16	3
p	1	3	4096	16
d	2	5	1048576	873

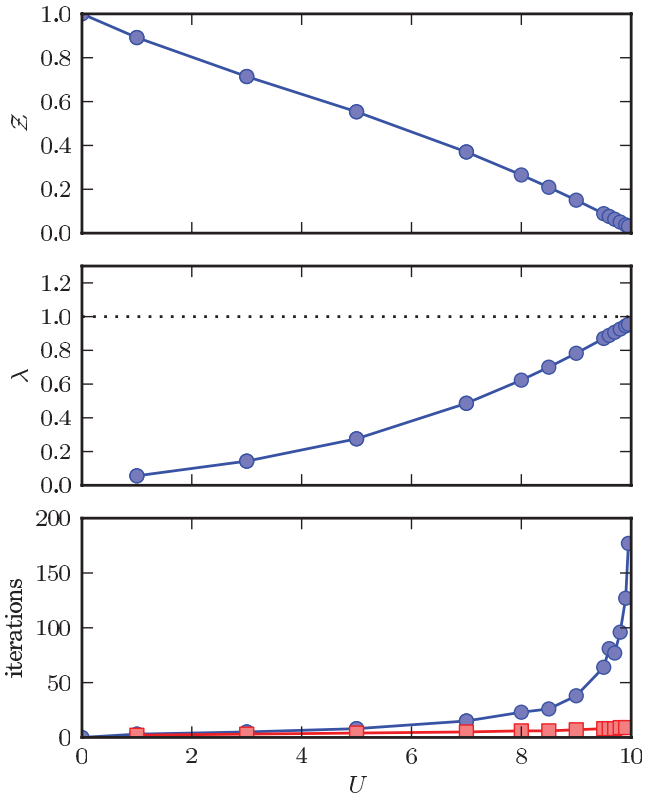

FIG. 6. (Color online) Convergence of the forward recursion scheme (circles) and of the Newton method (squares) for five bands at $N = 5$, $J = 0$, and $\Delta = 0$. The quasiparticle weight $\mathcal{Z} \equiv \mathcal{R}^2_{\alpha\alpha}$ goes to zero as U goes to the critical coupling $U_c \approx 10$. Simultaneously, the leading eigenvalue λ of the Jacobian of the recursion function goes to 1, and the number of forward iterations required to reach a fixed relative precision (here $|\mathcal{R}_i - \mathcal{R}_{i+1}| \leqslant 10^{-6}$ is used) diverges. On the contrary, the number of Newton iterations is almost independent of U. The matrix $[\mathcal{R}_0]_{\alpha\beta} = \delta_{\alpha\beta}$ is used as initial condition of both the forward recursion series and the Newton method $\forall U$.

complicated calculations, it may happen that the number of variational parameters is so large that the tensors cannot be stored in memory. In this case, it is still possible to calculate the traces "on the fly." This operation is trivially parallelizable.

It is well known that the speed of convergence of the forward recursion method [Eq. (87)] is limited by the magnitude of the largest eigenvalue λ of the Jacobian of the transformation $\mathcal{T}_{n^0}$ in the fixed point $\mathcal{R}$. In particular, if $|\lambda| \to 1$ the rate of convergence displays a critical slowing down. We have found that this situation actually occurs in our simulation when U approaches the Brinkman-Rice critical value. This is shown in Fig. 6, where the convergence of $\mathcal{R}$ is shown for different values of U at half-filling ($N = 5$), $J = 0$, and $\Delta = 0$. The value of λ was obtained as

$$\begin{aligned} \lambda &= \lim_{i\to\infty} (\mathcal{R}_{i+1} - \mathcal{R})/(\mathcal{R}_i - \mathcal{R}) \\ \mathcal{R} &= \lim_{i\to\infty} \mathcal{R}_i , \end{aligned} \tag{122}$$

where $\mathcal{R}_i$ was obtained from the forward recursion series [Eq. (87)] starting from the initial condition

$$[\mathcal{R}_0]_{\alpha\beta} = \delta_{\alpha\beta} \quad \forall U. \tag{123}$$

In DMFT the self-energy Σ is obtained as the solution of a fixed point problem,[6] analogously to the matrix $\mathcal{R}$, which is the solution of Eq. (88). It is known that also in DMFT the rate of convergence of the forward recursion method displays a critical slowing down in the vicinity of the Mott transition. This behavior has recently been shown to be related to the fact that the maximum eigenvalue of the Jacobian λ approaches 1 as U approaches the critical value,[54] as in our Gutzwiller calculations. In this case the convergence problem has been cured by employing quasi-Newton methods instead of the forward recursion scheme.[54,55] The same strategy is applicable to solve Eq. (88). As shown in Fig. 6, this strategy is very efficient. While the forward recursion algorithm slows down as U approaches its critical value, the number of required Newton iterations is essentially independent of U. The time required to calculate the results shown in Fig. 6 with the Newton method is less than 1 min for every single U. Nevertheless, the forward recursion method could be more stable in some case, as every forward recursion step leads to a decrease in total energy. In fact, see Sec. V, every evaluation of $\mathcal{T}_{n^0}$ corresponds to a minimization of the energy with respect to the Slater determinant followed by a minimization with respect to the Gutzwiller projector. This guarantees that the fixed points calculated by the forward-recursion method are local minima, while the Newton method can converge also to fix points with one or more Jacobian eigenvalues $|\lambda| > 1$, i.e., to stationary points of the energy that are not local minima.

We remark that the numerical procedure proposed in this paper is divided into two steps. (i) Construction of the functional $\mathcal{E}_{\text{var}}[n^0]$ optimizing the variational energy for a fixed variational density matrix n^0. This optimization can be reduced to the fixed point problem [Eq. (88)] and solved with the methods discussed above. (ii) Direct minimization of $\mathcal{E}_{\text{var}}[n^0]$ with respect to n^0. For completeness, this procedure is illustrated explicitly here for the bilayer Hubbard model

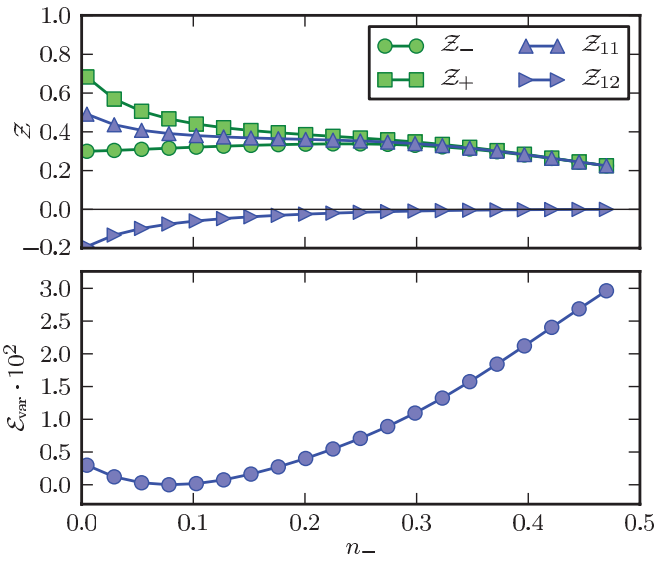

FIG. 7. (Color online) Sweep in the filling of the antibonding orbital n_- for the two-bands bilayer Hubbard model with equal bandwidths, local hybridization $V = 0.25$, filling $N = 1.88$, $U' = J' = J = 0$, and $U = 2.5$. Renormalization matrix $\mathcal{Z}$ (top panel) and total energy (bottom panel).

discussed in Sec. VII C. For each value of U the total energy $\mathcal{E}_{\text{var}}[n^0]$ was optimized with respect to the variational density n^0 using a bound minimization routine. An example is shown in Fig. 7, where the renormalization factors and the total energy are shown for fixed $U = 2.5$ and total filling per site $N = 1.88$ as a function of the antibonding orbital filling n_-. For each n_- the fixpoint problem of Eq. (88) was solved employing a quasi-Newton method with convergence criterion $|\mathcal{R}_i - \mathcal{R}_{i+1}| \leqslant 10^{-12}$ in less than 40 steps.

Finally, we point out that the presence of finite off-diagonal terms in $\mathcal{R}$ is due to the generality of the variational ansatz considered in this work. In fact, $\mathcal{R}$ is always diagonal if Eqs. (30) and (31) hold, as it was assumed in Ref. 20; see Sec. III C.

VIII. CONCLUSIONS

In this article we have derived a numerically efficient self-consistent implementation of the Gutzwiller variational method. The method proposed was obtained as a combination of the self-consistent numerical procedure recently derived by Deng *et al.* in Ref. 20 and the mathematical formulation of the Gutzwiller problem developed by Fabrizio and collaborators.[30,32–36] This formalism allows us to overcome the restriction to density-density interaction, which was assumed in Ref. 20, without increasing the complexity of the numerical algorithm. The approach drastically reduces the problem of the high-dimensional Gutzwiller minimization by mapping it to a minimization only in the variational density matrix, in the spirit of the Levy[38,39] and Lieb[40] formulation of DFT. For fixed density the Gutzwiller renormalization matrix is determined as a fixpoint of a proper functional of $\mathcal{R}$, whose evaluation only requires ground-state calculations of matrices defined in the Gutzwiller variational space. We have compared different methods to solve the fixpoint problem, finding that the Newton method is generally more efficient than the forward iteration method. The formalism also allows us to reduce the number of independent variational parameters in a well-controlled way using symmetries. As a proof of concept we have performed a few numerical calculations for two- and five-band Hubbard models with full rotationally invariant interaction, finding good agreement with available DMFT and slave-boson data. This analysis shows that the numerical approach derived is very stable and efficient. For these reasons this scheme is promising for first-principles studies of real materials, e.g., in combination with DFT (LDA + G).

It is noteworthy that the numerical implementation presented in this work allows for straightforward extensions in two directions of interest. (i) The variational freedom of the Gutzwiller wave function can be generalized in order to describe superconducting[32,34] and magnetic systems.[33] (ii) The assumption that the coefficients λ of the Gutzwiller projector [Eq. (4)] are real can be dropped and generalized to complex values. This allows, for instance, to account also for spin-orbit corrections to the on-site interaction.

ACKNOWLEDGMENTS

We are grateful to Michele Fabrizio and Giovanni Borghi for discussions. We also thank Frank Lechermann for

providing us with the slave-boson data in Figs. 2 and 5 and Philipp Werner for providing us with the DMFT data in Figs. 3 and 4. We acknowledge funding from the Mathematics-Physics Platform (MP^2) at the University of Gothenburg. The simulations were performed on resources provided by the Swedish National Infrastructure for Computing (SNIC) at Chalmers Centre for Computational Science and Engineering (C3SE) (project 001-10-37).

APPENDIX A: IRREDUCIBLE REPRESENTATION FOR A PARAMAGNETIC WAVE FUNCTION

In this Appendix we explain how to calculate the transformation V introduced in Eq. (53) for a general group G. Let us consider the example in which G is the symmetry group of a paramagnetic wave function invariant with respect to a specific discrete group of real (orbital) rotations $G_{\rm orb}$, e.g., the symmetry group of the cube. The problem consists in the definition of the most general ϕ matrix that commutes with the number operator $\hat{N}$, the representation of the spin $\hat{\mathbf{S}}$ and the representation $\hat{G}_{\rm orb}$ of $G_{\rm orb}$.

$$[\phi,\hat{N}] = [\phi,\hat{\mathbf{S}}] = [\phi,\hat{g}] = 0 \quad \forall \hat{g} \in \hat{G}_{\rm orb}. \tag{A1}$$

In order to achieve our purpose, the first step is to diagonalize simultaneously $\hat{N}$ and $\hat{\mathbf{S}}^2$. Each simultaneous eigenspace of these operators is the basis of a representation of the symmetry group G identified by the eigenvalues (N,S). We denote such a space $V_{N,S}$. Let us decompose $V_{N,S}$ in irreducible representations of the spin rotations. In order to do this we consider the kernel of the spin lowering operator $\hat{S}_-$ in $V_{N,S}$ and denote it by $V_{N,S,-S}$. We then calculate an orthonormal basis of $V_{N,S,-S}$ in which, for later convenience, $\hat{\mathbf{L}}^2$ and $\hat{L}_Z$ are also diagonal,

$$V_{N,S,-S} = \mathrm{Span}\left(\left\{\psi^{L,m_L,i}_{N,S,-S}\right\}\right). \tag{A2}$$

To each value of L, m_L, and i corresponds, by applying the raising $\hat{S}_+$ operator to $\psi^{L,m_L,i}_{N,S,-S}$ up to $2s$ times, a set of states labeled as $\{\psi^{L,m_L,i}_{N,S,m_S}\}$. Each subset $V^{L,m_L,i}_{N,S}$ is defined as

$$V^{L,m_L,i}_{N,S} = \mathrm{Span}\left(\left\{\psi^{L,m_L,i}_{N,S,m_S} \,\middle|\, m_s = -S,...,S\right\}\right) \tag{A3}$$

and is a basis of an irreducible representation of the spin group.

It is clear that, in order to commute with $\hat{N}$ and $\hat{\mathbf{S}}^2$, ϕ is decomposed in uncoupled blocks, each of them acting on the corresponding subspace $V_{N,S}$. In each block we group together the vectors $\{\psi^{L,m_L,i}_{N,S,m_S}\}$ with the same m_S. The Schur lemma[37] ensures that, if the above order convention is used, the (N,S) block of ϕ has the general form

$$\phi|_{V_{N,S}} = \begin{pmatrix} p^{N,S} & \cdots & 0 \\ \vdots & \ddots & \vdots \\ 0 & \cdots & p^{N,S} \end{pmatrix}. \tag{A4}$$

The structure of the matrix p in Eq. (A4) is further reduced by the condition $[\phi,\hat{G}_{\rm orb}] = 0$. The vector space V_{N,S,m_S} generated by $\{\psi^{L,m_L,i}_{N,S,m_S}\}_{L,m_L,i}$ is the basis of a representation of $G_{\rm orb}$, which can be decomposed in irreducible representations using standard methods. Notice, in fact, that a state $\psi^{L,m_L,i}_{N,S,m_S}$ transforms exactly as the spherical harmonic function $Y^L_{m_L}$ under rotations. Each one of the obtained irreducible representation of $G_{\rm orb}$ is labeled by its characters.[37] We group together all the equivalent representations with equal characters χ. This amounts to express V_{N,S,m_S} as the direct sum of V^{χ}_{N,S,m_S}. The Schur lemma[37] ensures that each one of the $p^{N,S}$ blocks defined in Eq. (A4) has the general form

$$p^{N,S} = \begin{pmatrix} q^{N,S}_{\chi_1} & \cdots & 0 \\ \vdots & \ddots & \vdots \\ 0 & \cdots & q^{N,S}_{\chi_{n_{\rm ch}}} \end{pmatrix}, \tag{A5}$$

where $n_{\rm ch}$ is the number of inequivalent representation in V_{N,S,m_S}.

The final step is to identify the n_k states of each subspace $V^{\chi_k}_{N,S,m_S}$ that belong to the same *row*[37] of the corresponding (equivalent) irreducible representations of $G_{\rm orb}$. The Schur lemma[37] restricts the structure of each $q^{N,S}_{\chi_k}$ block of Eq. (A5) as in Eq. (57), i.e.,

$$q^{N,S}_{\chi_k} = \begin{pmatrix} r^{N,S,\chi_k}_{11}\mathbb{1}_{d_k} & \cdots & r^{N,S,\chi_k}_{1n_k}\mathbb{1}_{d_k} \\ \vdots & \ddots & \vdots \\ r^{N,S,\chi_k}_{n_k1}\mathbb{1}_{d_k} & \cdots & r^{N,S,\chi_k}_{n_kn_k}\mathbb{1}_{d_k} \end{pmatrix}, \tag{A6}$$

where $\mathbb{1}_{d_k}$ are identity matrices of size $d_k \times d_k$ and d_k is the dimension of each one of the irreducible equivalent representations of $G_{\rm orb}$ repeated in $V^{\chi_k}_{N,S,m_S}$.

1. Proof of the assumption [Eq. (42)]

Let us prove that Eq. (42) is verified for every group G that does not mix configurations belonging to different eigenspaces of the number operator $\hat{N}$. We need two preliminary observations. (i) By assumption our uncorrelated wave function $|\Psi_0\rangle$ is invariant respect to the action of G, i.e.,

$$g|\Psi_0\rangle = e^{i\phi_g}|\Psi_0\rangle \quad \forall g \in G. \tag{A7}$$

(ii) From Eq. (37) we have that

$$D^\dagger(g)\bar{\rho}^0 D(g) = \bar{\rho}^0 \quad \forall g \in G, \tag{A8}$$

where

$$\bar{\rho}^0_{\alpha\beta} \equiv \langle\Psi_0| c^\dagger_\alpha c_\beta |\Psi_0\rangle \tag{A9}$$

is the variational density matrix expressed in the original basis; see Eq. (10). The density matrix $\bar{\rho}^0$ has exactly the same form of Eqs. (A4)–(A6) because of Eq. (A8). For this reason it can be diagonalized by means of a matrix $\mathcal{U}$ of the same form, i.e.,

$$D^\dagger(g)\mathcal{U}D(g) = \mathcal{U} \quad \forall g \in G. \tag{A10}$$

The single-particle transformations induced by the matrices $\mathcal{U}$ and $D(g)$ into the Fock many-body space evidently commute as a consequence of Eq. (A10). This concludes the proof of Eq. (42).

APPENDIX B: SELF-CONSISTENT FORMULATION OF THE ϕ-MATRIX OPTIMIZATION

We need to minimize the energy functional defined in Eq. (81) respect to the vector c fulfilling the Gutzwiller

constraints [Eqs. (82) and (83)]. The Gutzwiller constraints can be ensured by means of the following Lagrange functional

$$\mathcal{L}[c,\lambda] = \sum_{\alpha\beta} \lambda_{\alpha\beta} \langle c| N^S_{\alpha\beta} |c\rangle. \tag{B1}$$

The variation of $\mathcal{E}_{\Psi_0}[c]$ is given by

$$\begin{aligned}\delta\mathcal{E}[c] = {} & \langle \delta c| \sum_{\alpha\beta} \frac{\partial \langle \Psi_0| \hat{T}^G[\Psi_0,c] |\Psi_0\rangle}{\partial \mathcal{R}_{\alpha\beta}} \frac{M^S_{\alpha\beta}}{\sqrt{n^0_\beta(1-n^0_\beta)}} |c\rangle \\ & + \langle c| \sum_{\alpha\beta} \frac{\partial \langle \Psi_0| T^G[\Psi_0,c] |\Psi_0\rangle}{\partial \mathcal{R}_{\alpha\beta}} \frac{M^S_{\alpha\beta}}{\sqrt{n^0_\beta(1-n^0_\beta)}} |\delta c\rangle \\ & + \langle \delta c|U |c\rangle + \langle c|U |\delta c\rangle, \end{aligned} \tag{B2}$$

and the variation of the Lagrange functional [Eq. (B1)] is given by

$$\delta\mathcal{L}[c,\lambda] = \langle \delta c| \sum_{\alpha\beta} \lambda_{\alpha\beta} N^S_{\alpha\beta} |c\rangle + \langle c| \sum_{\alpha\beta} \lambda_{\alpha\beta} N^S_{\alpha\beta} |\delta c\rangle. \tag{B3}$$

The condition that the variation of

$$\delta\mathcal{F}_{\Psi_0}[c,\lambda] \equiv \delta\mathcal{E}_{\Psi_0}[c] + \delta\mathcal{L}[c,\lambda] = 0 \quad \forall \delta c \perp c \tag{B4}$$

is equivalent to the following "nonlinear eigenvalue problem"

$$F_{\Psi_0}[c,\lambda]|c\rangle = E|c\rangle, \tag{B5}$$

where

$$\begin{aligned} F_{\Psi_0}[c,\lambda] = {} & U + \sum_{\alpha\beta} \frac{\partial \langle \Psi_0| \hat{T}^G[\Psi_0,c] |\Psi_0\rangle}{\partial \mathcal{R}_{\alpha\beta}} \frac{M^S_{\alpha\beta}}{\sqrt{n^0_\beta(1-n^0_\beta)}} \\ & + \sum_{\alpha\beta} \lambda_{\alpha\beta} N^S_{\alpha\beta}. \end{aligned} \tag{B6}$$

In principle, the minimization of $\mathcal{E}_{\Psi_0}[c]$ could be performed recursively, starting from a given "guess" c_0 and iterating the following eigenvalue problem

$$F_{\Psi_0}[c_n,\lambda_n]|c_{n+1}\rangle = E_{n+1}|c_{n+1}\rangle, \tag{B7}$$

where E_{n+1} is the lowest eigenvalue of $F_{\Psi_0}[c_n,\lambda_n]$ and λ_n are the Lagrange multipliers such that c_{n+1} satisfies the Gutzwiller constraints. The minimum of $\mathcal{E}_{\Psi_0}[c]$ is realized in

$$c_{\min} = \lim_{n\to\infty} c_n. \tag{B8}$$

Instead, to calculate $c_{\min}$, it is convenient to approximate $c_{\min}$ with c_1. This approximation can be considered as the result of a "linearization" of the functional $\mathcal{E}_{\Psi_0}[c]$ around the initial guess c_0.

APPENDIX C: NUMERICAL IMPLEMENTATION OF THE TIGHT-BINDING PROBLEM

Let us consider a general translational invariant noninteracting tight-binding Hamiltonian

$$\hat{H} = \hat{T} + \Delta\hat{H}, \tag{C1}$$

where

$$\hat{T} = \sum_{\alpha\beta} \sum_{\mathbf{R}\neq\mathbf{R}'} t^{\alpha\beta}_{\mathbf{R}\mathbf{R}'} d^\dagger_{\mathbf{R}\alpha} d_{\mathbf{R}'\beta}, \tag{C2}$$

$$\Delta\hat{H} = \sum_{\alpha\beta} \delta^{\alpha\beta} \sum_{\mathbf{R}} d^\dagger_{\mathbf{R}\alpha} d_{\mathbf{R}\beta}. \tag{C3}$$

The translational invariance of the system

$$t^{\alpha\beta}_{\mathbf{R}\mathbf{R}'} = t^{\alpha\beta}_{\mathbf{R}+\mathbf{R}_0\,\mathbf{R}'+\mathbf{R}_0} \quad \forall\, \mathbf{R}_0, \alpha, \beta \tag{C4}$$

allows us to express $\hat{H}$ in k space

$$\hat{H} = \sum_{\alpha\beta} \sum_{\mathbf{k}} \left(t^{\alpha\beta}_{\mathbf{k}} + \delta^{\alpha\beta}\right) d^\dagger_{\mathbf{k}\alpha} d_{\mathbf{k}\beta}, \tag{C5}$$

where

$$t^{\alpha\beta}_{\mathbf{k}} = \sum_{\mathbf{R}} e^{-i\mathbf{k}\mathbf{R}} t^{\alpha\beta}_{\mathbf{R}\mathbf{0}}. \tag{C6}$$

From Eq. (C5) $\hat{H}$ can be easily diagonalized numerically and expressed in terms of its eigenoperators as follows:

$$\hat{H} = \sum_{\mathbf{k}n} \epsilon_{\mathbf{k}n}\, \eta^\dagger_{\mathbf{k}n} \eta_{\mathbf{k}n}. \tag{C7}$$

Notice that the overlap matrix

$$(U_{\mathbf{k}})_{\alpha n} = \langle 0|\, d_{\mathbf{k}\alpha} \eta^\dagger_{\mathbf{k}n} |0\rangle \tag{C8}$$

appears in Eq. (75).

[1] M. C. Gutzwiller, Phys. Rev. Lett. **10**, 159 (1963).
[2] M. C. Gutzwiller, Phys. Rev. **134**, A923 (1964).
[3] M. C. Gutzwiller, Phys. Rev. **137**, A1726 (1965).
[4] H. Yokoyama and H. Shiba, J. Phys. Soc. Jpn. **56**, 1490 (1987).
[5] M. Capello, F. Becca, M. Fabrizio, S. Sorella, and E. Tosatti, Phys. Rev. Lett. **94**, 026406 (2005).
[6] A. Georges, G. Kotliar, W. Krauth, and M. J. Rozenberg, Rev. Mod. Phys. **68**, 13 (1996).
[7] W. Metzner and D. Vollhardt, Phys. Rev. Lett. **59**, 121 (1987).
[8] W. Metzner and D. Vollhardt, Phys. Rev. B **37**, 7382 (1988).
[9] F. Gebhard, Phys. Rev. B **41**, 9452 (1990).
[10] E. Müller-Hartmann, Z. Phys. B **76**, 211 (1989).
[11] W. F. Brinkman and T. M. Rice, Phys. Rev. B **2**, 4302 (1970).
[12] M. Dzierzawa, D. Baeriswyl, and S. M. Martelo, Helv. Phys. Acta **70**, 124 (1997).
[13] N. Lanatà, Phys. Rev. B **82**, 195326 (2010).
[14] M. Schirò and M. Fabrizio, Phys. Rev. Lett. **105**, 076401 (2010).
[15] N. Lanatà and U. R. Strand (2011), e-print arXiv:1102.2741 [cond-mat].
[16] P. Hohenberg and W. Kohn, Phys. Rev. **136**, B864 (1964).
[17] W. Kohn and L. J. Sham, Phys. Rev. **140**, A1133 (1965).
[18] O. Gunnarsson and B. I. Lundqvist, Phys. Rev. B **13**, 4274 (1976).
[19] K. M. Ho, J. Schmalian, and C. Z. Wang, Phys. Rev. B **77**, 073101 (2008).

[20]X. Y. Deng, L. Wang, X. Dai, and Z. Fang, Phys. Rev. B **79**, 075114 (2009).
[21]V. I. Anisimov, F. Aryasetiawan, and A. Lichtenstein, J. Phys. Condens. Matter **9**, 767 (1997).
[22]G. Kotliar, S. Y. Savrasov, K. Haule, V. S. Oudovenko, O. Parcollet, and C. A. Marianetti, Rev. Mod. Phys. **78**, 865 (2006).
[23]J. Bünemann, W. Weber, and F. Gebhard, Phys. Rev. B **57**, 6896 (1998).
[24]J. Kanamori, Proj. Theor. Phys. **30**, 275 (1963).
[25]P. Werner, E. Gull, and A. J. Millis, Phys. Rev. B **79**, 115119 (2009).
[26]T. A. Costi and A. Liebsch, Phys. Rev. Lett. **99**, 236404 (2007).
[27]P. Werner, E. Gull, M. Troyer, and A. J. Millis, Phys. Rev. Lett. **101**, 166405 (2008).
[28]J. Bünemann and W. Weber, Phys. Rev. B **55**, 4011 (1997).
[29]Z. Gulácsi, R. Strack, and D. Vollhardt, Phys. Rev. B **47**, 8594 (1993).
[30]C. Attaccalite and M. Fabrizio, Phys. Rev. B **68**, 155117 (2003).
[31]Q.-H. Wang, Z. D. Wang, Y. Chen, and F. C. Zhang, Phys. Rev. B **73**, 092507 (2006).
[32]M. Fabrizio, Phys. Rev. B **76**, 165110 (2007).
[33]N. Lanatà, P. Barone, and M. Fabrizio, Phys. Rev. B **78**, 155127 (2008).
[34]N. Lanatà, P. Barone, and M. Fabrizio, Phys. Rev. B **80**, 224524 (2009).
[35]M. Ferrero, F. Becca, M. Fabrizio, and M. Capone, Phys. Rev. B **72**, 205126 (2005).
[36]N. Lanatà, Ph.D. thesis, SISSA-Trieste (2009).
[37]E. P. Wigner, *Group Theory and Its Application to the Quantum Mechanics of Atomic Spectra* (Academic Press, New York, 1959).
[38]M. Levy, Proc. Natl. Acad. Sci. USA **76**, 6062 (1979).
[39]M. Levy, Phys. Rev. A **26**, 1200 (1982).
[40]E. Lieb, Int. J. Quantum Chem. **24**, 243 (1983).
[41]M. T. Heath, *Scientific Computing An Introductory Survey*, 2nd ed. (McGraw-Hill, New York, 2002).
[42]G. Borghi, M. Fabrizio, and E. Tosatti, Phys. Rev. B **81**, 115134 (2010).
[43]F. Lechermann, A. Georges, G. Kotliar, and O. Parcollet, Phys. Rev. B **76**, 155102 (2007).
[44]S. E. Barnes, J. Phys. F **6**, 1375 (1976).
[45]S. E. Barnes, J. Phys. F **7**, 2637 (1977).
[46]P. Coleman, Phys. Rev. B **28**, 5255 (1983).
[47]N. Read and D. M. Newns, J. Phys. C **16**, 3273 (1983).
[48]G. Kotliar and A. E. Ruckenstein, Phys. Rev. Lett. **57**, 1362 (1986).
[49]J. Bunemann and F. Gebhard, Phys. Rev. B **76**, 193104 (2007).
[50]J. Bünemann, F. Gebhard, and R. Thul, Phys. Rev. B **67**, 075103 (2003).
[51]A. Koga, Y. Imai, and N. Kawakami, Phys. Rev. B **66**, 165107 (2002).
[52]P. Werner and A. J. Millis, Phys. Rev. Lett. **99**, 126405 (2007).
[53]A. M. Läuchli and P. Werner, Phys. Rev. B **80**, 235117 (2009).
[54]H. U. R. Strand, A. Sabashvili, M. Granath, B. Hellsing, and S. Östlund, Phys. Rev. B **83**, 205136 (2011).
[55]R. Zitko, Phys. Rev. B **80**, 125125 (2009).